Final report on in-reactor creep-fatigue deformation behaviour of a CuCrZr alloy: COFAT 1

Singh, Bachu Narain; Tähtinen, S.; Moilanen, P.; Jacquet, P.; Dekeyser, J.; Edwards, D.J.; Li, M.; Stubbins, J.F.

Publication date:
2007

Document Version
Publisher's PDF, also known as Version of record

RISØ

Risø-R-Report

Final Report on In-Reactor Creep-Fatigue Deformation Behaviour of a CuCrZr Alloy: COFAT 1

B.N.Singh, S.Tähtinen, P.Moilanen, P. Jacquet, J. Dekeyser, D.J. Edwards, M. Li and J.F. Stubbins

Risø-R-1571(EN)

Risø National Laboratory
Technical University of Denmark
Roskilde, Denmark
August 2007

DTU

Author: B.N. Singh [1)], S. Tähtinen[2)], P. Moilanen[2)], P. Jacquet[3)], J. Dekeyser[3)], D.J. Edwards[4)], M. Li[5)] and J.F. Stubbins[6)]
Title: Final Report on In-reactor Creep-fatigue Deformation Behaviour of a CuCrZr Alloy: COFAT 1
Department: Materials Research Department

[1)] Materials Research Department, Risø National Laboratory, DK-4000 Roskilde, Denmark
[2)] VTT Industrial Systems, Fin-02044 VTT, Finland
[3)] Reactor Technology Design Department, SCK·CEN, 200 Boeretang, B-2400 Mol, Belgium
[4)] Materials Structure and Performance Group, Pacific Northwest National Laboratory, Richland, WA99352, USA
[5)] Materials Science and Technology Division, Oak Ridge National Laboratory, Oak Ridge, Tennessee, USA
[6)] Department of Nuclear, Plasma and Radiological Engineering, University of Illinois, Urbana, Illinois, USA

Risø-R-1571(EN)
August 2007

Abstract

At present, practically nothing is known about the deformation behaviour of materials subjected simultaneously to external cyclic force and neutron irradiation. The main objective of the present work is to determine experimentally the mechanical response and resulting microstructural changes in CuCrZr(HT1) alloy exposed concurrently to flux of neutrons and creep-fatigue cyclic loading directly in a fission reactor. Special experimental facilities were designed and fabricated for this purpose. A number of in-reactor creep-fatigue experiments were successfully carried out in the BR-2 reactor at Mol (Belgium). In the present report we first describe the experimental facilities and the details of the in-reactor creep-fatigue experiments carried out at 363 and 343K at a strain amplitude of 0.5% with holdtimes of 10 and 100s, respectively. For comparison purposes, similar creep-fatigue tests were performed outside of the reactor. (i.e. in the absence of neutron irradiation).

During in-reactor tests, the mechanical response was continuously registered throughout the whole test. The results are first presented in the form of hysteresis loops confirming that the nature of deformation during these tests was truly cyclic. The temporal evolution of the stress response in the specimens is presented in the form of the average maximum stress amplitude as a function of the number of cycles as well as a function of displacement dose accumulated during the tests. The results illustrate the nature and magnitude of cyclic hardening as well as softening as a function of the number of cycles and displacement dose. Details of the microstructure were investigated using TEM and STEM techniques. The fracture surface morphology was investigated using SEM technique. Both mechanical and microstructural results are briefly discussed. The main conclusion emerging from the limited amount of present results is that neither the irradiation nor the duration of the holdtime have any significant effect on the lifetime (in terms of number of cycle to failure) of the material.

ISSN 0106-2840
ISBN 87-550-3538-8

Contract no.:
TW3-TVM-COFAT 1

Group's own reg. no.: 1610013-00

Sponsorship: EU – Fusion Technology Programme

Cover :

Pages: 45
Tables: 2
References: 17

Information Service Department
Risø National Laboratory
Technical University of Denmark
P.O.Box 49
DK-4000 Roskilde
Denmark
Telephone +45 46774004
bibl@risoe.dk
Fax +45 46774013
www.risoe.dk

Contents

1. Introduction

At present it seems almost certain that the precipitation hardened CuCrZr alloy will be used both in the first wall and divertor components of the International Thermonuclear Experimental Reactor (ITER). In service, both these components will be exposed to an intense flux of fusion (14MeV) neutrons and will experience at the same time thermo-mechanical cyclic loading (i.e. fatigue) as a result of the cyclic nature of plasma burn operations of the system. Consequently, the structural materials in the reactor vessel will have to endure not only the cyclic loading but also the stress relaxation and microstructural recovery (i.e. creep) during the "plasma-on" and "plasma-off" periods.

In an effort to evaluate the impact of cyclic loading (fatigue) on mechanical performance of CuCrZr alloy, the low cycle fatigue behaviour was investigated at temperatures in the range of 295 to 623 K both in the unirradiated and the neutron-irradiated conditions [1,2]. Recently, the creep-fatigue deformation behaviour of CuCrZr alloy has been studied extensively both in the unirradiated and the neutron- irradiated conditions at 295 and 573 K [3]. In these studies, the effects of holdtime and strain amplitudes were investigated. The results of these investigations exhibited a general tendency that the application of holdtime during creep-fatigue loading practically always reduces the number of cycles to failure. Another interesting feature illustrated by these results was that the effect of creep-fatigue loading on fatigue life increases with decreasing strain amplitude. These effects of creep-fatigue mode of deformation on the lifetime of CuCrZr alloy remain rather elusive and at present no clear and reliable explanation can be advanced.

The nature of deformation is likely to get even more complex during creep-fatigue loading in the environment of energetic neutrons because of continuous production of lattice defects and their clusters. These defect and defect clusters would interact with the deformation-induced dislocations. As a result, both dislocation dynamics and defect accumulation are likely to get modified. These modifications would directly affect the mechanical performance of the structural materials during creep-fatigue deformation in a fusion reactor like ITER. To our knowledge, practically nothing is known at present either experimentally or theoretically about the nature of plastic deformation and its impact on the mechanical performance and lifetime of CuCrZr alloy under the complicated conditions of concurrent creep-fatigue loading and neutron irradiation. It is relevant to note here that at least the fatigue behaviour of the CuCrZr alloy has been investigated during irradiation with 600 MeV protons [4].

In view of the above described complications involved in the in-reactor deformation experiments, it must be recognized that the results of out-of-rector creep-fatigue experiments on the unirradiated or irradiated materials are totally inadequate for describing the in-reactor deformation behaviour.

It is therefore essential, at least in our view, to perform well controlled creep-fatigue experiments directly in a reactor to determine the dynamic response of the material when it is exposed concurrently to external force (producing dislocations) and to the flux of neutrons (generating lattice defects and their clusters) as a function of the

number of creep-fatigue cycle (and irradiation dose). On the basis of these results, a realistic and reliable assessment of mechanical response and lifetime of materials can be made for the case of creep-fatigue loading in the environment of neutrons in a fission or/and fusion reactor.

Recently an experimental facility has been developed jointly by VTT (Finland), SCK.CEN (Belgium) and Risø National Laboratory (Denmark) specifically to study the deformation behaviour and its impact on mechanical response and lifetime of materials during creep-fatigue loading in the environment of fission neutrons. In this test facility provisions are made to implement holdtime both in the tensile and compression sides of the cyclic tests. In the following we first describe briefly the experimental facility designed and constructed for carrying out in-reactor creep-fatigue tests (section 2). The results of both out-of-reactor and in-reactor creep-fatigue tests and microstructural investigations are described in section 3 and are briefly discussed in section 4. Section 5 presents the summary and main conclusions of the present work.

2. Materials and Experimental Procedure

2.1 Materials

The material used in the present investigations was a precipitation hardened CuCrZr alloy supplied by Outokumpu Oyj (Finland) with a composition of Cu-0.73% Cr-0.14% Zr. The alloy was solution annealed at 1233 K for 3 hours, water quenched and then prime aged at 733K for 3 hours. After this heat treatment the material was water quenched again. Finally, the prime aged material was overaged at 873K for 1 hour and then water quenched. Henceforth this heat treatment will be referred to as HT1. The main purpose of this heat treatment was to coarsen the precipitates so that they could be stronger obstacles to dislocation motion during deformation.. The final grain size after HT1 heat treatment was found to be 60μm. The size and geometry of the specimens used in the in-reactor creep-fatigue tests are shown in Figure 1(a). A photograph of one of the specimens used in these tests is shown in Figure 1(b).

2.2 Test module and irradiation rig

In order to carry out in-reactor creep-fatigue tests, a special test facility was designed and constructed. The facility consists of a pneumatic fatigue test module and a servo-controlled pressure-adjusting loop. The pressure-adjusting loop operates on a continuous flow of helium gas. The basic principle of the creep-fatigue test module is based on the use of two pneumatic bellows, one to introduce tensile and the other one to introduce compressive stress / strain on the specimen. A linear variable differential transformer (LVDT) sensor is used to measure the resulting extension of the gauge length of the creep-fatigue specimen during the deformation. The strain measured in the gauge length of the specimen is used to control the pre-determined strain amplitude throughout the whole creep-fatigue test. It should be pointed out that the strain measured by the LVDT is calibrated against the strain measured by strain gauges during the out-of-reactor creep-fatigue tests. Details of the design of creep-fatigue test modules and the procedure for calibrating the stress and strain measured in these modules are described in a separate report [5]. The outside diameter of the test module was 50mm and the total length of the module together with the LVDT was 250mm. The accuracy of the load

calibration was found to be ± 1% of the actual value of the stress resulting from the applied pressure causing the displacement in the specimen.

A number of modules were tested for their functional performance and reliability before finalizing the design. The detailed design and geometry of the module were then adjusted to make it compatible with the irradiation conditions in the BR-2 reactor at Mol.

To accommodate the test modules and the necessary instrumentation to be able to perform the creep-fatigue tests in the reactor, special irradiation rigs were designed and constructed at Mol. Figure 2(a) shows the simplified layout and operational features of the test module including the instrumentation. The photograph in Figure 2(b) shows the final assembly of two test modules, two specimens and the necessary instrumentation. The whole assembly is loaded in the irradiation rig which is hung in a thimble tube. During the whole test period, the irradiation rig remained submerged in the demineralised reactor pool water. However, to avoid overheating of the specimens due to gamma heating the pool water was circulated in the irradiation rig at a rate of 600 litres per hour from the top of the test assembly. This means that the cold water flowing in the rig first cools the test module on the top of the assembly and somewhat warmer water flowing down the rig cools the test module at the bottom of the assembly. As a result, the specimen in the test module at the top of the assembly would be expected to remain at somewhat lower temperature than the specimen in the test module at the bottom of the assembly. The temperature profile in each test module was measured by three thermocouples placed at three different positions (i.e. LVDT, specimen and bellow) in the rig. (Figure 2). Three dosimeters were placed at the specimen level to measure the neutron fluence.

2.3 In-reactor creep-fatigue tests

The irradiation rig was designed to accommodate two complete test modules so that two independent creep-fatigue tests can be performed at the same time. In addition, a subsize fatigue specimen was attached to each test module which was irradiated in unstressed condition but with the same neutron flux and at the same temperature as for the in-reactor creep-fatigue test.

The irradiation rig containing the assembly of specimens, LVDTs, cooling system and thermocouples was lowered in the reactor core when the local neutron flux near the rig had reached a steady state level after the reactor start. The rig was manually inserted into the open tube at position G60 of BR-2 reactor core. As the rig was lowered in the open tube, the temperature of the test modules increased rapidly due to the gamma heating power of $2Wg^{-1}$. It took about 10 minutes to reach a stable temperature in the modules 1 and 2 of 343 and 363K, respectively. The test module 1 was situated at the top and the test module 2 at the bottom of the assembly in the rig. As expected, the temperature in the test module 1 remained about 20K lower than that in the test module 2 throughout the whole test period. The temperature of each test module was measured and recorded separately and continuously. The temperature measured on the test module was taken to be the temperature of the specimen.

The creep-fatigue cyclic loading was initiated almost immediately after the temperature in the test modules had stabilized. The test on the specimen in module 2 was identified as Test No.1 and on the specimen in the module 1 as Test No.2. Both tests

were carried out in the strain controlled mode with a strain amplitude of 0.5 %. The loading cycles were always fully reversed (i.e. R=-1) so that the maximum strain in the tension side of the cycle was the same as the maximum strain on the compression side of the cycle. Time taken to reach from pull to push (i.e. tension to compression) was 50s both in Test No.1 and 2, giving a strain rate of $2x10^{-4}$ s^{-1} during the loading period. In the case of Test No. 1, a holdtime of 10s was implemented both in the tension and compression sides of the fatigue cycles. A holdtime of 100s was used in the Test No.2. All the relevant test parameters used in these tests are summarized in Table 1. During the creep-fatigue tests the evolution of the stress and strain in the specimen was continuously recorded. The stress acting on the specimen was determined from the measured value of the gas pressure in the bellows and the magnitude of the strain was obtained from the measured value of extension of the gauge length of the specimen by LVDT sensors attached to the specimen.

Table 1. Test parameters for in-reactor creep-fatigue experiments in BR-2 reactor

Test Parameters	Test No.1	Test No.2
Strain amplitude (%)	0.5%	0.5%
Holdtime in tension and compression (s)	10	100
Total time per complete cycle (s)	120	300
Neutron flux (n/m^2s (E>0.1 MeV))	$6.5x10^{17}$	$7.4x10^{17}$
Damage rate (dpa/s)	$6.1x10^{-8}$	$7.2x10^{-8}$
Irradiation and test temperature (K)	363±1	343±1
Displacement dose at the start of creep-fatigue test (dpa)	$3.7x10^{-5}$	$5.6x10^{-5}$
Displacement dose per cycle (dpa)	$7.32x10^{-6}$	$2.16x10^{-5}$
Displacement dose during deformation (dpa)	0.0166	0.054
Total displacement dose experienced by the specimen (dpa)	0.0457	0.054

2.4 Microstructural investigations

The microstructure of CuCrZr alloy used in the present creep-fatigue experiments was investigated in the following states: (a) unirradiated and undeformed, (b) unirradiated and deformed, (c) irradiated and undeformed and (d) irradiated and deformed concurrently with a strain amplitude of 0.5% and with a holdtime of 10s (Test No.1) and 100s (Test No.2). For the transmission electron microscopy (TEM) examinations, 3mm diameter discs were obtained from the gauge length of the creep-fatigue specimens. In cases where specimens broke during the test, the disc was taken from the portion of the gauge length closest to the fractured surface. Prior to electropolishing, the discs were mechanically polished down to a thickness of ~120µm. Thin foils for TEM investigations were prepared by twin-jet electropolishing in a solution of 25 % phosphoric acid, 25 % ethylene glycol and 50 % water at 9.5 V for about 2 min. at ~293K. Thin foils were examined in a JEOL 2000FX transmission

electron microscope. The surface morphology of the fractured specimens was investigated using a JEOL 5310 LV scanning electron microscope (SEM).

3. Experimental Results

Before describing the results on microstructural evolution and deformation behaviour during the in-reactor creep-fatigue tests, it is crucially important to point out that the experimental conditions during these tests are fundamentally different from those existing during the conventional out-of-reactor tests on the unirradiated or post-irradiated materials. In the conventional tests both the microstructural evolution and the deformation behaviour are entirely dependent on the stress-induced generation of dislocations, their interactions with each other and with-other microstructrural features such as precipitates, particles and irradiation- induced defect clusters that may provide resistance to dislocation motion. This relatively simple situation is, however, likely to get significantly complicated during the in-reactor deformation experiments. The complications would arise due to the fact that during the in-reactor experiments the generation of stress-induced dislocations and neutron-induced defects and defect clusters would occur concurrently. Consequently, the mobile defects and their clusters would contaminate (e.g. decorate) both the grown-in and freshly generated dislocations, modifying the intrinsic dislocation mobility. In addition, the production and accumulation of sessile defect clusters (e.g. loops and stacking fault tetrahedra) would present additional obstacles to dislocation motion.

In view of these complications, caution should be exercised in assessing the results of the in-reactor experiments and comparing them with the results of out-of-reactor conventional deformation experiments. Furthermore, in order to be able to rationalize the results of the in-reactor experiments and to be able to draw some reasonable conclusions from the results, it is very important to establish the details of the microstructure and deformation behaviour of the unirradiated reference material in the undeformed and deformed (out-of-reactor) states. Therefore, these details are presented in the following subsection (subsection 3.1) before describing the results on the in-reactor deformation behaviour and the resulting microstructure at the end of the in-reactor creep-fatigue tests (subsection 3.2).

3.1 Microstructure and mechanical properties prior to irradiation

The dominating feature of the microstructure of the overaged CuCrZr (HT 1) alloy (in unirradiated and undeformed condition) as revealed by the TEM investigation was the presence of a relatively high density of small Cr-rich precipitates. The spatial distribution of these precipitates was found to be fairly homogenous throughout the whole grains and there were no significant variations in the size and density of precipitates from grain to grain. Figure 3 shows the general feature of the precipitate microstructure. The average precipitate size and density in the overaged and unirradiated CuCrZr (HT1) alloy were found to be 8.7 nm and 1.7 x 10^{22} m^{-3}, respectively [6]. It is worth mentioning that in the overaged specimen of CuCrZr (HT1) alloy, some of the grain boundaries were found to contain a low density of relatively large (100 – 150 nm) precipitates.

Since lifetime of CuCrZr alloy during creep-fatigue deformation is likely to be affected by the yield strength of the alloy [3], tensile test was performed on the overaged CuCrZr (HT 1) alloy. The tensile test was carried out at 353K at a strain rate of ~10^{-5} s^{-1} using the same size and geometry of the specimen as used in the in-reactor creep-fatigue tests. The test was performed in a test module identical to the one used in the in-reactor tests. The resulting stress-strain curve is shown in Figure 4.

Prior to carrying out in-reactor creep-fatigue tests, the creep-fatigue deformation behaviour of the unirradiated CuCrZr (HT 1) alloy was determined by performing out-of-reactor tests at 353K. These tests were carried out using the same specimen size and geometry, the same test module and the same test parameters as used in the in-reactor creep-fatigue tests (section 2.3). Figure 5(a) shows the measured temporal evolution of the strain and stress response of the specimen during the first five cycles of the test carried out with a strain amplitude of 0.5 % and with a holdtime of 100s both in the tension and compression sides of the cycles. It should be noted that as expected the strain level during the holdtime remains constant (at 0.5 %) since the test is carried out in the strain controlled mode. The stress level, on the other hand, fluctuates and decreases slightly during the holdtime. This is expected to occur because of the relaxation of the dislocation microstructure during the holdtime period. The variation of the maximum stress level (both in tension and compression) with the number of cycles indicates that the maximum stress level increases with the increasing number of cycles suggesting that the material hardens somewhat during the first few cycles of the creep-fatigue test.

Figure 5 (b) shows the cyclic deformation behavior in the form of hysteresis loops illustrating the dynamic stress-strain relationship during the creep-fatigue test described in Figure 5 (a). These loops describe the deformation behaviour during those first five cycles of the creep-fatigue test shown in Figure 5 (a). The stability and the symmetry of the hysteresis loops shown in Figure 5 (b) confirm the true cyclic nature of deformation during the creep-fatigue test.

In order to illustrate the stability of the cyclic nature of deformation throughout the whole creep-fatigue test, a number of hysteresis loops for the higher number of creep-fatigue cycles representing increasingly higher level of deformation are shown in Figure 6. The position and shape of the loops indicate that the cyclic deformation remains stable during the first 500 cycles of the test and becomes clearly unstable beyond about 1000 cycles.

The average value of the maximum stress reached in the tension and compression sides of a deformation cycle (i.e. the stress amplitude) is plotted in Figure 7 as a function of number of cycles during the out-of reactor creep-fatigue test at 353K with a strain amplitude of 0.5 % and with a holdtime of 100s. It can be seen in Figure 7 that the material hardens during the first 50 – 60 cycles of the creep-fatigue test. The hardening seems to saturate at about 100 cycles and remains saturated until about 1000 cycles beyond which the specimen begins to soften and shows the sign of instability.

The post-deformation microstructure of the CuCrZr (HT1) specimen out-of-reactor creep-fatigue tested at 353K was investigated using TEM. The TEM discs were obtained from the region close to the fractured surface. The TEM examination showed that the post-deformation microstructure was quite uniform throughout the whole volume examined and was composed of precipitates, dislocation segments and some relatively small loops. (Figure 8). Most of the dislocation segments were rather short in length with

varying degree of curvature. The microstructure showed no indication of build-up of dislocation density in the form of dislocation walls.

3.2 In-reactor creep-fatigue deformation behaviour

3.2.1 Mechanical response

As indicated in section 2.3, the evolution of stress and strain during in-reactor creep-fatigue tests was continuously recorded. The measured temporal evolution of strain and stress response of the specimen during the first five cycles of the in-reactor creep-fatigue test on CuCrZr (HT1) specimen with a strain amplitude of 0.5% and a holdtime of 10s (Test No.1) is shown in Figure 9(a). The test parameters used in the experiments are quoted in Table 1. The results shown in Figure 9(a) clearly suggest that the peak value of the measured stress levels both in the tension and compression sides of the cycle increases with increasing number of cycles. In other words, the specimens hardens slightly during each loading cycle. The strain level, on the other hand, remains constant during each cycle simply because the test is performed in strain-controlled mode. It should be noted that no significant amount of stress relaxation occurs during the holdtime period of 10s neither in the tension nor in the compression side of the loading cycle.

The cyclic deformation behaviour in the form of hysteresis loops is shown in Figure 9(b) illustrating the dynamic stress-strain relationship during the creep-fatigue Test No.1. The loops shown in Figure 9(b) describe the deformation behaviour during those first five cycles of the creep-fatigue test shown in Figures 9(a). The stability and the symmetry of the hysteresis loops shown in Figure 9(b) confirm that during the in-reactor test the true cyclic nature of deformation is achieved and maintained. It should be noted that the peak value of the stress level reached in the tension side of the cycles is slightly higher that in the compression side. The reason for this asymmetry is not quite obvious at present.

Figure 10 shows the results of the in-reactor creep-fatigue Test No. 2 carried out on CuCrZr (HT1) specimen also with a strain amplitude of 0.5% but with a holdtime of 100s. The irradiation and test temperature in this case was 343K. The temporal evolution of strain and stress response during this test is shown in Figure 10(a) for the first five cycles of the cyclic loading. Just like in the case of Test No.1 (Figure 9(a)), the measured peak stress levels both in the tension and compression sides of the cycle increases with increasing number of cycles, indicating hardening of the material during each loading cycle (Figure 10(a)). The measured stress response (Figure 10(a)) clearly illustrates the occurrence of stress relaxation during the holdtime. The reason for the jerky nature of the stress relaxation during the holdtime is not clear at present. It should be noted, however, that the magnitude of the stress relaxation is rather small.

The dynamic stress-strain relationship during the cyclic loading for the first five cycles during the Test No.2 is shown in Figure 10(b) in the form of hysteresis loops.The stability and the continued symmetry of these hysteresis loops confirm once again that during the in-reactor creep-fatigue test (Test No.2) a proper cyclic nature of deformation is achieved and maintained during the test. It should be noted that during this test the peak value of the stress level reached in the tension side of the cycle is practically the same as in the compression side of the cycle.

Since both Test No.1 and 2 were carried out until the end of life of specimens (see section 2.3), a number of hysteresis loops for the higher number of creep-fatigue cycles during Test No.1 and 2 are shown in Figure 11. The position and the symmetry of hysteresis loops clearly show that a proper cyclic nature of deformation is maintained during the whole test period of the in-reactor Test No.1 and 2. It should be noted that the hysteresis loops for the cycle number 2000 both in Test No.1 and 2 clearly show a sharp drop in the stress amplitude indicating the presence of major cracks in the specimens.

The variation of the maximum stress amplitude measured in the in-reactor tests (Test No.1 and 2) is shown in Figure 12 as a function of (a) number of cycles and (b) displacement dose level. The maximum stress amplitude is the average value of the peak stress reached in the tension and compression sides of a loading cycle. For comparison purposes, the results of out-of-reactor creep-fatigue test carried out at 353K with a strain amplitude of 0.5% and a holdtime of 100s are also shown in Figure 12(a). The following features of the results shown in Figure 12(a) are worth noting: (a) the material hardens with the number of cycle during in-reactor tests(Test No.1 and 2) as well as during out-of-reactor test, (b) the magnitude of hardening during Test No.1 and 2 is almost identical, (c) the level (i.e. the magnitude) of hardening during the in-reactor tests(Test No. 1 and 2) is higher than that during the out-of-reactor test, (d) the rate of hardening per cycle during the in-reactor tests and the out-of-reactor test is practically the same, the hardening comes to saturate at about 100 cycles during in-reactor tests as well as during out-of-reactor test and (e) the specimens during the in-reactor tests (No. 1 and 2) begin to show sign of softening already beyond about 100 cycles whereas in the case of the out-of-reactor test the onset of softening does not occour until beyond about 1000 cycles.

In order to examine the impact of continuous production of defects and their clusters by fission neutrons on the mechanical response of the specimens during creep-fatigue cycle loading, the measured maximum stress amplitude is plotted against displacement dose in Figure 12(b) for Test No.1 and 2. Even though the rate of increase in hardening with increasing dose level is very similar in Test No.1 and 2 at low doses (i.e. up to about $1x10^{-4}$ dpa in Test No.1 and $2x10^{-4}$ dpa in Test No.2) the magnitude of hardening at a given dose level is clearly higher in the Test No.1 than that in the Test No.2. up to a dose level of about $4x10^{-4}$ dpa. At a dose level of about $6x10^{-4}$ dpa, the stress level in the Test No.1 and 2 is almost identical. The increase in hardening with increasing the dose level decreases with dose and comes to saturate at a dose level of about 10^{-3} dpa in the case of Test No. 2. The level of maximum hardening reached in Test No.2 is slightly higher than that in the Test No. 1. It is interesting to note that the specimens during the in-reactor creep-fatigue Tests No1 as well as the Test No.2 suffer from considerable level of softening during a large fraction of their total liftetime.

Photographs of the fractured parts of the specimens used in the in-reactor creep-fatigue (a) Test No1 and (b) Test No.2 are shown in Figure 13. It should be noted that these specimens did not break into pieces during the actual tests in the reactor. In fact they broke in the hot cells during the removal of the specimens from the test modules. It is also worth noting that these specimens did not show any sign of necking prior to fracture.

3.2.2 Microstructure and fracture surface morphology

To help understand the mechanical response of CuCrZr (HT1) alloy during in-reactor creep-fatigue tests reported in the preceeding section (3.2.1), the microstructure

of the specimens used in Test No. 1 and Test No. 2 was investigated using TEM and STEM (scanning transmission electron microscopy) techniques. It is worth noting here, however, that the results of these investigations provide information about the microstructure only at the end of the in-reactor tests. In other words, the nature of the microstructural evolution as a function of the number of creep-fatigue cycles or the increasing level of displacement dose remains unknown. In spite of this limitation, however, the details of the microstructure even at the end of the in-reactor tests provide very valuable information about physical processes operating during cyclic deformation. In this section we first report the defect microstructure accumulated in the CuCrZr (HT1) specimen during irradiation alone, i.e. in the absence of concurrent plastic deformation. This is followed by the results on various aspects of the microstructure that has survived in the specimens at the end of the in-reactor Test No. 1 and Test No. 2. Finally, the results of fracture surface morphology investigations are briefly described.

In order to establish the impact of deformation induced mobile dislocations on the accumulation of defect clusters produced concurrently during in-reactor creep-fatigue tests, it is crucially important to determine the damage accumulation in the absence of dislocation generation (i.e. without plastic deformation). To achieve this goal, TEM discs were taken from the end of the "head" of the creep-fatigue specimen used in the in-reactor Test No. 2. Since the diameter of the specimen "head" is 3 times larger than the gauge diameter (see Figure 1a), the stress acting on this part of the specimen will be only one-nineth of the stress experienced by the gauge section of the specimen. Thus, the discs used for TEM investigations did not experience at any time during the in-reactor Test No. 2 stress beyond the yield stress (see Figure 4) of the material. Hence the damage accumulation observed in these discs may be considered to have occurred in the absence of deformation-induced mobile dislocations. It should be noted here that the irradiation conditions (i.e. damage rate, irradiation temperature and displacement dose level) for these TEM discs, on the other hand, were identical to those experienced by the material of the gauge section of the specimen used in the in-reactor Test No. 2.

The microstructure of CuCrZr (HT1) specimen used in the Test No. 2 irradiated at 343K to a displacement dose level of 0.054 dpa (but not deformed) is illustrated in Figure 14. A relatively low magnification micrograph shown in Figure 14(a) illustrates that the microstructure containing SIA (self-interstitial atom) loops and SFTs (stacking fault tetrahedral) has evolved in a homogeneous fashion. Note that the microstructure in figure 14(a) also contains a homogeneous distribution of precipitates (see Figure 3). The specimen also contained a modest density of discrete and clearly resolveable SIA loops (Figure 14(b)). The average size and density of loops are similar to the results reported earlier [7] for pure copper irradiated at 373K to a dose level of 0.01 dpa. Figure 14(c) shows the precipitates and SFTs. A number of such micrographs were used to determine the size distributions and average size and density of precipitates and SFTs. The average size and density of precipitates and SFTs are quoted in Table 2. The average size and density of SFTs are comparable to the results published earlier for pure copper irradiated at 373K to dose levels of 0.01 and 0.1 dpa [7].

Figure 15 shows surviving defect microstructure (eg. precipitate and SFTs) in specimens used in the in-reactor creep-fatigue test (a) at 363K with a holdtime of 10s

(Test No. 1) and (b) at 343K with a holdtime of 100s (Test No. 2), respectively. It should be noted that because of a holdtime of only 10s, the specimen in the Test No. 1 fractured already at a dose level of 0.0166 dpa. The specimen in the Test No. 1 remained exposed to the neutron flux, however, until the specimen was removed from the reactor core at the final dose level of 0.0457 dpa (see Table 1). This means that the microstructure in specimen used in Test No. 1 evolved under the impact of stress only for about one-third of the time it was exposed to neutrons. In other words, the damage accumulation in this specimen took place for the two-third of the time without any influence of the applied stress. The microstructural evolution in the specimen used in the Test No. 2, on the other hand, took place under the influence of applied stress during the whole test period. Thus, the microstructure observed in the specimen used in the Test No. 2 should represent the microstructure truly characteristic of the microstructure affected by the concurrent application of neutron damage and plastic deformation.

Table 2. SFT and precipitate size and density in the in-reactor creep-fatigue tested CuCrZr (HT1) specimens

In-reactor test	Test Temp. (K)	Dose (dpa)	Size (nm)		Density (m^{-3})	
			SFT	Ppt.	SFT	Ppt.
Test No. 1	636	0.046	2.5	7.2	$3.4x10^{23}$	$1.5x10^{22}$
Test No. 2	343	0.054	2.6	7.0	$1.6x10^{23}$	$2.8x10^{22}$
Test No. 2 undeformed*)	343	0.054	2.8	6.4	$4.4x10^{23}$	$1.3x10^{22}$

*) the TEM discs were taken from the end of the “head” of the specimen used in the in-reactor creep-fatigue Test No. 2.

The size distributions of precipitates and SFTs were determined from the measurements on TEM micrographs taken from specimens (a) irradiated but undeformed, (b) in-reactor Test No. 1 and (c) in-reactor Test No. 2. The results are shown in Figure 16 and 17. The average size and density of SFTs for these different conditions are quoted in Table 2. The results shown in Figure 16 and Table 2 clearly suggest that neither irradiation nor irradiation and deformation have any significant impact on precipitate size and density. The SFT average size in all three cases are found to be almost identical. It is interesting to note, however, that the SFT size distributions and the densities in the three cases are noticeably different. The SFT densities in the in-reactor deformed specimens both in the case of the in-reactor Test No. 1 and Test No. 2 are found to be lower than that in the case of irradiated but undeformed specimen. It should be noted that the SFT density in the case of irradiated and undeformed specimen is very similar to the density reported earlier for pure copper irradiated at 373K to 0.1 dpa [7]. As pointed out earlier, the case of the in-reactor Test No . 1 is complicated by the fact that the damage accumulation in this experiment has occurred for a considerable period of time in the absence of plastic deformation. It is therefore impossible to

determine as to how much of this reduction in SFT density in the case of the in-reactor Test No. 1 is due to deformation. In the case of the in-reactor Test No. 2, it is reasonable to argue, on the other hand, that the reduction in SFT density might be due to dynamic nature of highly mobile dislocations and their interactions with SFTs during in-reactor creep-fatigue deformation. It should be noted that during this experiment the entire damage accumulation has occurred under the influence of concurrent damage production and cyclic deformation.

In order to investigate the dislocation microstructure in the in-reactor creep-fatigue tested specimens used in the Test No. 1 and test No. 2, TEM specimens were prepared from the material immediately adjacent to the fracture surface of the in-reactor tested specimens. TEM examination showed the presence of a rather low density of short dislocation segments.Neither dislocation net-work nor segregation of dislocations into dislocation walls were observed. Figure 18 (a) shows the dislocation microstructure in the specimens surviving at the end of the Test No. 1 reaching a displacement dose level of 0.0457 dpa (see Table 1). The microstructure is dominated by the homogeneously distributed small loops and only a few isolated short dislocation segments could be seen. Most of the dislocation segments appear to be associated with small loops. It is worth pointing out that in some parts of the specimens some loose groups of dislocation segments and loops were present. An example is shown in Figure 18(b). Here again, most of the segments are found to be associated with loops.

The dislocation microstructure in the specimen used in the in-reactor Test No. 2 was found to be very similar to that observed in the case of the Test No. 1. No accumulation of dislocations produced during creep-fatigue deformation were observed in the form of dislocation net-work or dislocation walls. Figure 19(a) shows the post-deformation microstructure which is dominated by homogeneously distributed dislocation loops and a relatively low density of short dislocation segments invariably decorated by the dislocation loops. In some areas of the specimen, some long dislocation segments were observed again mostly decorated by some small loops (Figure 19(b)). There was, however, no indication of dislocation-dislocation interaction and tangle formation. In this specimen too some dislocations were found in the form of loose groups of dislocation segments that appear to be heavily decorated by small loops (Figure 19(c)).

Thicker portions of the TEM discs obtained from the specimens used in the in-reactor Test No. 1 and Test No. 2 were examined using STEM technique. These examinations revealed the evidence for localised deformation in the form of bands in the specimen used in the Test No. 1 as well as Test No. 2. These bands have the appearance as well as features of “cleared channels” commonly observed in specimens tensile tested either in-reactor or post-irradiation out-of-reactor tests (e.g. [8]). It should be mentioned that the clear channels have also been observed in the post-irradiation fatigue tested specimens of CuCrZr alloy [2]. Since the cleared channels observed in the present experiments contain some residual defect clusters and loops, we shall call them “diffuse” clear channels (DCCs). Figure 20 shows a STEM micrograph taken from the specimen used in the in-reactor Test No. 1. A number of DCCs are clearly visible and they appear to have eminated from a grain boundary. The width of DCCs varies between about 100 and 200 nm. Examples of DCCs observed in the specimen used in the in-reactor Test No. 2 are shown in Figure 21. These micrographs were also taken in the STEM mode. A similar example of a DCC taken in the TEM mode is shown in Figure 22. It can be seen in Figure 22 that some short dislocation segments and SIA loops have survived in the

DCC. It is also worth pointing out that DCCs in the specimen deformed in the Test No. 2 (see Figure 21) are considerably wider than those observed in the Test No. 1 (see Figure 20). The width of DCCs shown in Figures 21 and 22 varies between about 600 and 800 nm.

As mentioned earlier, unlike the cleared channels in the post-irradiation tensile tested specimens that are found to contain no defect clusters, in the present experiments some defect clusters (e.g. SFTs) do manage to survive in the DCC. The TEM micrograph presented in Figure 23(a) shows the presence of SFTs in very low density in the middle of a DCC. The Cr-rich precipitates are also clearly visible in the micrograph. For comparison, Figure 23(b) shows the SFT and precipitate microstructure immediately adjacent to the DCC. The micrographs presented in Figures 23(a) and 23(b) were taken from the specimen used in the in-reactor Test No. 2. The density of SFTs in Figure 23(b) is very similar to the value of the average density of SFTs measured in this specimen (Table 2).

The fracture surfaces of in-reactor and out-of-reactor creep-fatigue tested specimens were examined by scanning electron microscopy. A series of fractographs were taken of the whole fracture surface of each specimen starting from the crack initiation point near the specimen surface to the final fracture point near the other surface of the specimen along the crack propagation direction. An overview of the fracture surface for the unirradiated and out-of-reactor creep-fatigue tested specimen is shown in Figure 24. The out-of-reactor creep-fatigue test was carried out at 353K at a strain amplitude of 0.5% with a holdtime of 100s. Similar overviews of the fracture surface for the in-reactor creep-fatigue specimens used in the Test No 1. and Test No. 2 are shown in Figures 25 and 26, respectively. Enlarged fractographs showing fatigue striations in the area where striations became first visible and also in the area prior to final fracture are also given for each specimen in Figure 24, 25 and 26 to show the development of fatigue striations.

The fractographic morphology of fracture surfaces (Figures 24, 25 and 26) was quite similar for all three specimens. The fatigue process operating in these specimens can be characterised by three distinct stages, i.e. stage I, crack initiation (featureless fractographs), stage II, crack growth (fatigue striations) and stage III, fast ductile fracture. A single crack initiation zone near the specimen edge was observed for all test conditions. The stage II propagation fracture surface is marked by well-defined fatigue striations (e.g. Figures 24 and 26) and occupies a substantial fraction of the total fracture surfaces in the out-of-reactor as well as in the in-reactor tested (Test No. 2) specimens. It is interesting to note that in the specimen creep-fatigue tested out-of-reactor, the striation spacing increases with increasing number of cycles (i.e. with increasing crack length) indicating an increasing crack growth rate (Figure 24). In the case of the in-reactor tested (Test No. 2) specimen, on the other hand, the striation spacing remained practically unchanged with increasing number of cycles (Figure 26) (i.e. increasing crack length) indicating a constant crack growth during the whole crack growth period (i.e. stage II).

From the enlarged fractographs shown in Figures 24 and 26, it is possible to estimate the striation spacing. Then, assuming that there is one-to one correlation between the striation spacing and the crack propagation in a single cycle (i.e. each striation is caused by one full strain cycle), the crack growth rate during the out-of reactor and the in-reactor tests (Test No. 2) can be obtained. The estimate of the crack growth rate based on this procedure yields a crack growth rate of 7.5×10^{-3} mm/cycle

which is very high and is well into stage II crack growth for the out-of-reactor test as well as for the in-reactor Test No. 2.

4. Discussion

While considering the mechanical response results shown in Figure 12(a), it is relevant to point out that the evolution of the stress amplitude measured in the out-of-reactor test is very similar to the results obtained on the same material in the conventional creep-fatigue tests published earlier [3]. This provides an additional assurance that both in-reactor and out-of-reactor creep-fatigue tests carried out in the present work using specially fabricated test modules are reliable and provide results that are in agreement with the ones determined using conventional test machine.

The main features of the results presented in Figure 12(a) are listed in subsection 2.3.1 and will not he repeated here. There are, however, some aspects of the results shown in Figure 12(a) and (b) that deserve further comments. For instance, even though the effect of irradiation on the hardening level becomes noticeable already during the first creep-fatigue cycle, the rate of hardening per cycle in the out-of-reactor test and in the in-reactor tests No. 1 and 2 is practically the same (Figure 12(a)). This means that even though the accumulated displacement dose level in the in-reactor tests increases with the increasing number of creep-fatigue cycles, the increase in the magnitude af hardening per cycle does not change. The results presented in Figure 12(b) show that in the hardening regime, the hardening level at a given dose level in the case of the in-reactor test No. 2 remains lower than that in the case of the in-reactor Test No. 1. This is simply because the number of cycles at a given dose level in the case of Test No. 1 is nearly three times larger than that in the case of Test No. 2. Furthermore, the results presented in figure 12 show that the number of cycles at which the hardening level comes to saturate is insensitive to irradiation as well as holdtimes. Thus, it would appear that it is really the number of creep-fatigue cycles which is the most potent parameter controlling the mechanical response of the material in the hardening regime.

It is worth pointing out that the increase in the hardening level already during the first cycle of the in-reactor Test No. 1 and 2 may be partly due to the accumulation of defect clusters and partly due to decoration of grown-in dislocations by small SIA loops. As indicated in Table 1, the dose levels at the start of the first creep-fatigue cycle in the Test No. 1 and 2 are 3.7×10^{-5} and 5.6×10^{-5} dpa, respectively. In pure copper, for example, the cluster densities at these dose levels have been found to be $\sim 5 \times 10^{21} m^{-3}$ and $\sim 1 \times 10^{22} m^{-3}$ [9]. The presence of these clusters would be expected to cause hardening [10] already in the first cycle. Recent analytical calculations have shown that at these dose levels the grown-in dislocations are likely to acquire dense enough decoration of SIA loops to be able to cause significant amount of hardening [11]. Thus, it is quite feasible that both of these factors may contribute to the initial hardening during the in-reactor creep-fatigue tests.

Beyond the first creep-fatigue cycle the problems of damage accumulation and the resulting mechanical response become very complex because of (a) production and recovery of deformation induced mobile dislocations, (b) continuous production of radiation induced defects, (c) interactions between mobile and pinned dislocations and

glissile and sessile defect clusters causing dislocation decoration, absorption of defect clusters into dislocation core and (d) the drag of defect clusters by dislocations moving at relatively high velocity under the applied stress. As a result of these events the microstructural evolution and the corresponding mechanical response will remain in transitional state until a quasi-steady-state is reached after a certain number of creep-fatigue cycles. Since nothing is known about the state of the microstructure as a function of the number of cycles, it is practically impossible at present to provide any reasonable and reliable explanation as to why the rate of hardening per cycle does not increase with increating number of cycles (and increasing displacement dose level). For the same reason, nothing much can be said as to why the hardening in the in-reactor tests saturates almost at the same number of cycles as in the case of the out-or-reactor test. In-reactor interrupted creep-fatigue tests may provide answers to these important questions.

It is interesting to note that beyond the saturation in hardening, the deformation in the out-of-reactor test continues at the same maximum stress amplitude until about 1000 cycles and then the stress level decreases rapidly leading to final failure of the specimen. In the in-reactor tests Test No. 1 and 2, on the other hand, specimens begin to soften already after about 100 cycles first slowly and then rapidly beyond about 1000 cycles, leading to final failure of the specimens.

The results described in the subsection 3.2.2 provide some useful insight into the microstructural evolution processes during the in-reactor creep-fatigue experiments. First of all, it is worth mentioning that the SFT size and density measured in the irradiated (but undeformed) CuCrZr(HT1) alloy at 343K to a dose level of 0.054 dpa (Test No. 2) (Table 2) are very similar to the values reported earlier for OFHC-copper [7] and CuCrZr alloy [12] irradiated at 373K to doses of 0.1 and 0.3 dpa, respectively. It is also worth pointing out that neither the irradiation alone nor the irradiation and simultaneous deformation affect the precipitate size and density (Figure 16 and Table 2). These results are consistent with earlier results showing that neutron irradiation at 320K up to 0.2 dpa does not affect the size and density of precipitates in the CuCrZr alloy [13]. The results shown in Figure 17 and Table 2 do strongly suggest, however, that the size distribution and density of SFTs are markedly affected by the in-reactor creep-fatigue deformation particularly during the Test No. 2. It should be noted that the example of the Test No. 2 is very clear and clean one since during this experiment simultaneous irradiation and deformation took place throughout the whole life of the experiment.

It is logically reasonable to interprete the decrease in SFT density in the in-reactor deformed specimen in Test No. 2 in terms of removal of some of the SFTs continuously being produced during the Test No. 2 by the interaction of mobile population of dislocations and SFTs (see later for further evidence). In this context it is also of interest to note that the homogeneous distribution of discrete SIA loops observed in the corresponding irradiated and undeformed specimen (also from Test No. 2) (Figure 14(b)) was found to be absent in the in-reactor deformed specimen in Test No. 2. This would indicate removal of SIA loops also by mobile dislocations during the cyclic deformation. This means that during the in-reactor creep-fatigue tests while the irradiation produces continuously new SFTs and SIA clusters, the production and motion of dislocations during the cyclic loading keeps removing a certain fraction of the SFTs and SIA clusters. The impact of this dynamic process would have to be included in the consideration of the mechanical response in terms of cyclic hardening, the saturation of hardening and the cyclic softening.

The suggestion that during the in-reactor deformation experiments, some of the irradiation induced SIA loops and SFTs may get removed by interaction with mobile dislocations is consistent with the results of molecular dynamics simulations [14, 15], dislocation dynamics simulation [16] and analytical calculations [14]. The removal of small SIA loops occurs by their absorption into the core of the interacting dislocations. The removal of SFTs by gliding dislocations, on the other hand, is more complicated. Molecular dynamics simulations have shown that the interaction of a gliding dislocation with SFTs causes either partial absorption or shearing of SFTs [15]. Both molecular dynamics simulations [17] and analytical calculations [11] have shown, on the other hand, that under an applied stress gliding dislocations can drag the SIA loops decorating them. These loops being dragged at a relatively high velocity may interact with SFTs causing their shrinkage and annihilation.

TEM examinations of the out-of-reactor tested specimen (in the unirradiated state) as well as specimens used in the in-reactor creep-fatigue Tests No. 1. and 2 revealed that at the end of these tests only a few isolated dislocation lines had survived. Furthermore, in these specimens there were no signs of dislocation segregation in the form of dislocation walls. In the case of the unirradiated specimens, the end of life microstructure was composed mainly of short dislocation segments (Figure 8). In the case of the in-reactor deformed specimens both the isolated dislocation segments (Figures 18(a) and 19(a) and groups of short segments (Figures 18(b) and 19(b) were found to be decorated by small loops. At present no clear explanation can be given for the absence of a proper dislocation microstructure in specimens deformed in the unirradiated (out-of-reactor test) and irradiated (in-reactor test) conditions.

It is significant that the specimens tested in the in-reactor Test No. 1 as well as Test No. 2 provide the evidence for localization of deformation in the form of DCC (diffuse clear channel) (Figures 20 and 21). At present simple and no credible explanation can be provided as to when and why DCCs are formed. The fact that the density of SFTs and other defect clusters (i.e. SIA loops etc.) is considerably lower in the middle of these DCCs than in the matrix just outside of the DCCs would suggest that a significant number of dislocations have passed through the DCCs. In other words, a number of dislocations must have been generated at the sources of these DCCs.

If we assume that these DCCs will have similar impact on the mechanical performance and lifetime of the material as the cleared channels have in the case of in-reactor tensile tests [8], then one may suspect that the formation and growth of DCCs may play an important role in determining the level of cyclic hardening, saturation in hardening followed by softening and the lifetime of the specimens during the in-reactor creep-fatigue tests. In order to substantiate this proposition, however, we need to know as to when and where these DCCs are formed. This can be achieved only by carrying out a number of in-reactor “interrupted” creep-fatigue tests.

5. Summary and conclusions

The present work has demonstrated that well defined and controlled creep-fatigue deformation experiments can be successfully carried out in a fission reactor. The validity of the experimental results obtained during in-reactor creep-fatigue tests has been established so that these results can be compared with the results obtained in conventional creep-fatigue tests carried out using standard mechanical testing machines

outside of a reactor. The stability and the symmetry of the hysteresis loops have confirmed the true cyclic nature of deformation during the in-reactor creep-fatigue tests.

Both in-reactor and out-of-reactor creep-fatigue tests were carried out using specially designed test modules on an overaged CrCrZr (HT1) alloy at temperatures in the range of 343 and 363K. Tests were performed at a strain amplitude of 0.5% with a holdtime of 10s or 100s both in the tension and compression sides of the cycles. The displacement damage rates during in-reactor tests were 6.1×10^{-8} dpa/s (Test No. 1) and 7.2×10^{-8} dpa/s (Test No. 2).

Both in-reactor and out-of-reactor tests exhibit cyclic hardening during the first 50-60 cycles, the level of hardening being higher in the in-reactor tests than that in the out-of-reactor tests. Surprisingly, the rate of hardening per cycle, however, is almost identical in both kinds of tests. Furthermore, in both kinds of tests the hardening comes to saturate at about 50-60 cycles. In the case of the out-of-reactor test the maximum stress amplitude remains almost constant up to about 1000 cycles. The in-reactor tests, on the other hand, exhibit softening already beyond only about 100 cycles inspite of continuous irradiation.

The number of cycles to failure is found to be about the same (within a factor of about two) for the in-reactor tests and the out-of-reactor test, indicating that neither the irradiation nor the length of holdtime has any significant effect on the lifetime of the specimens during creep-fatigue deformation.

Microstructural investigations have shown that “diffuse” cleared channels (DCCs) are formed in the in-reactor creep-fatigue tested specimens. The width of DCCs is generally noticeably larger in the specimen tested with 100s holdtime than that in the specimen tested with 10s holdtime. Neither the in-reactor nor the out-of-reactor tested specimens show the presence of many residual dislocations. No evidence of dislocation segregation in the form of dislocation walls were found in these specimens.

A quantitative characterization of the irradiation-induced SFTs in the as-irradiated (and undeformed) and irradiated and simultaneously deformed (i.e. in-reactor tested) specimens has shown that the density of SFTs in the in-reactor deformed specimens is lower than that in the irradiated and undeformed specimens. In view of the results of analytical calculations and molecular dynamics simulations the reduction in the density of SFTs is interpreted to be due to removal of SFTs as a result of their interaction with SIA loops dragged by the gliding dislocations under the influence of applied stress during the in-reactor deformation experiments.

The limited amount of available microstructural information makes it almost impossible to say much about as to why and when the DCCs are formed and as to what role do they play in the nucleation and growth of cracks and thus in determining the lifetime of the specimens.

The analysis of the fractography results suggests that both in the in-reactor tests and in the out-of-reactor test the specimens spent about 20% their lifetime in producing a visible crack which then grew in a stable manner with increasing number of cycles. It is somewhat surprising, however, that the irradiation does not seem to affect this behaviour.

Acknowledgements

The present work was partly funded by the European Fusion Technology Programme. The authors would like to thank a number of technical staff members at VTT, Mol and Risø for their valuable help in carrying out the present experiments.

References

[1] B.N. Singh, J.F. Stubbins and P. Toft, Risø-R-991(EN), May (1997), 42 p.

[2] B.N. Singh, J.F. Stubbins and P.Toft, Risø-R-1128(EN), March (2000), 55 p.

[3] B.N. Singh, M.Li, J.F Stubbins and B.S. Johansen, Risø-R-1528(EN), August (2005), 55 p.

[4] P.Marmy, J. Nucl. Mater. 329 -333 (2004) 188 .

[5] P. P.Moilanen, S. Saarela, S. Tähtinen, B.N. Singh and P. Jacquet, VTT Research Report No. VTT-R-09316-06, 21 December 2006, 25 p.

[6] B.N. Singh, D.J. Edwards and S. Tähtinen, Risø Report No. RISØ-R-1436(EN), December (2004), 24p.

[7] B.N. Singh, D.J. Edwards and P. Toft, J.Nucl.mater. 299 (2001) 205.

[8] B.N. Singh, D.J. Edwards, S. Tähtinen, P. Moilanen, P. Jacquet and J. Dekeyser, Risø-R-1481(EN), October (2004), 46p.

[9] B.N. Singh and S..J. Zinkle, J.Nucl.Mater., 206 (1993) 212.

[10] S.J. Zinkle and L.T. Gibson, DOE-ER-0313/27, December 31 (1999) 163.

[11] H. Trinkaus and B.N. Singh, Risø Report No. Risø-R-1610 (EN) (2007), in preparation.

[12] D.J. Edwards, B.N. Singh, Q. Xu and P. Toft, J.Nucl.Mater. 307-311 (2002) 439.

[13] B.N. Singh, D.J. Edwards and P. Toft, J.Nucl.Mater. 238 (1996) 244.

[14] D. Rodney and G. Martin, Phys.Rev. B, 61 (2000) 8714.

[15] Y.N. Osetsky, D. Rodney and D.J. Bacon, Phil.Mag. 86 (2006) 2295.

[16] N.M. Ghoniem, S.-H. Tong, B.N. Singh and L.Z. Sun, Phil.Mag. A 81 (2001) 2743.

[17] Y.N. Osetsky, D.J. Bacon, Z. Rong and B.N. Singh, Phil.Mag. Letters, 84 (2004) 754.

(a)

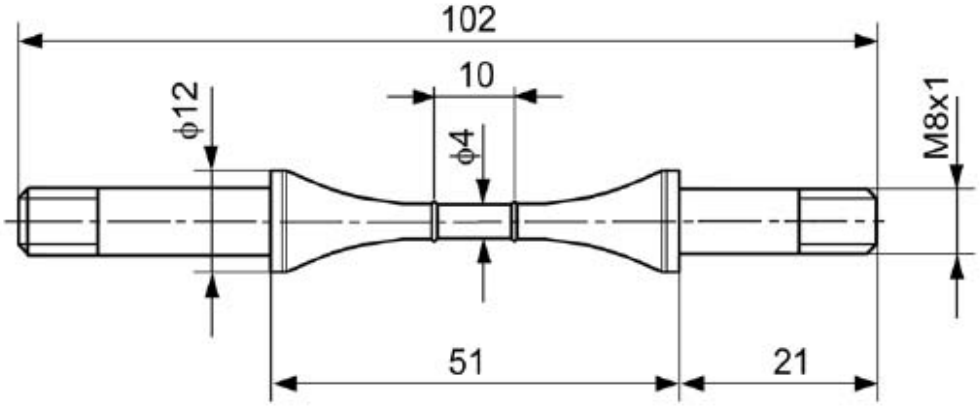

(b)

Figure 1. (a) Size and geometry of the creep-fatigue specimens used in the out-of-reactor and in-reactor creep-fatigue tests and (b) a photograph of one of the creep-fatigue specimens used in these tests.

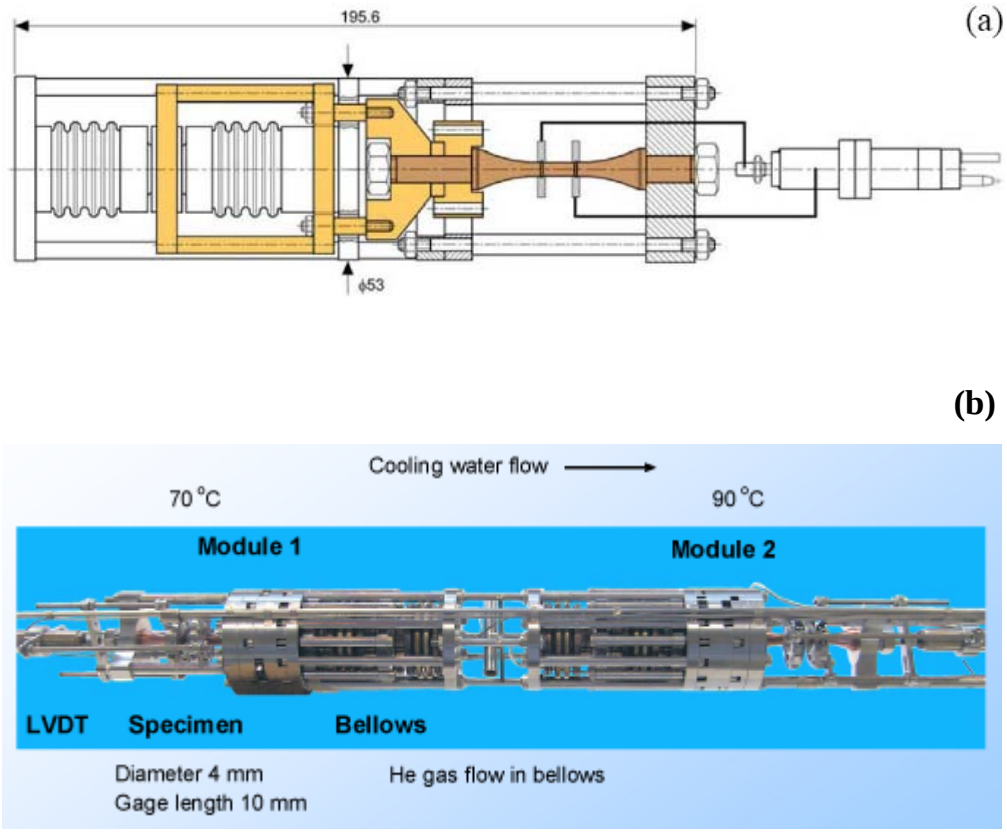

Figure 2. (a) Simplified layout and operational features of the test module and (b) the final assembly of the two complete test modules in the instrumented irradiation rig.

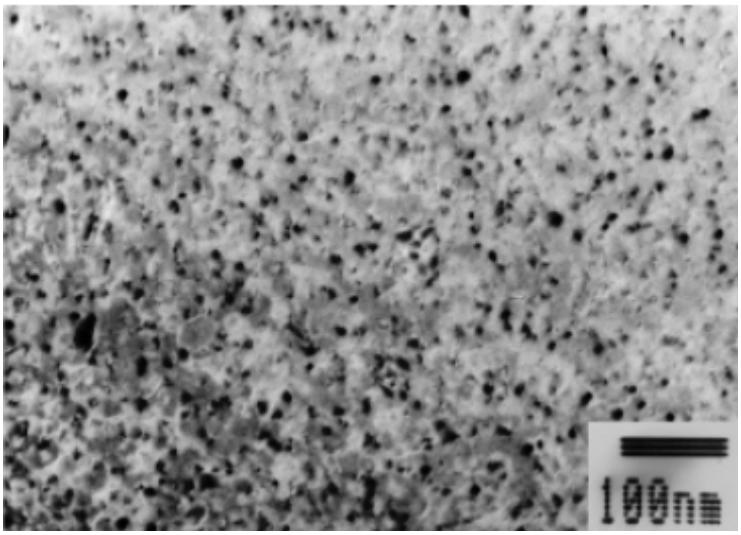

Figure 3. (a) Transmission electron micrograph showing precipitate microstructure of the unirradiated and undeformed CuCrZr alloy in the overaged(HT1) condition.

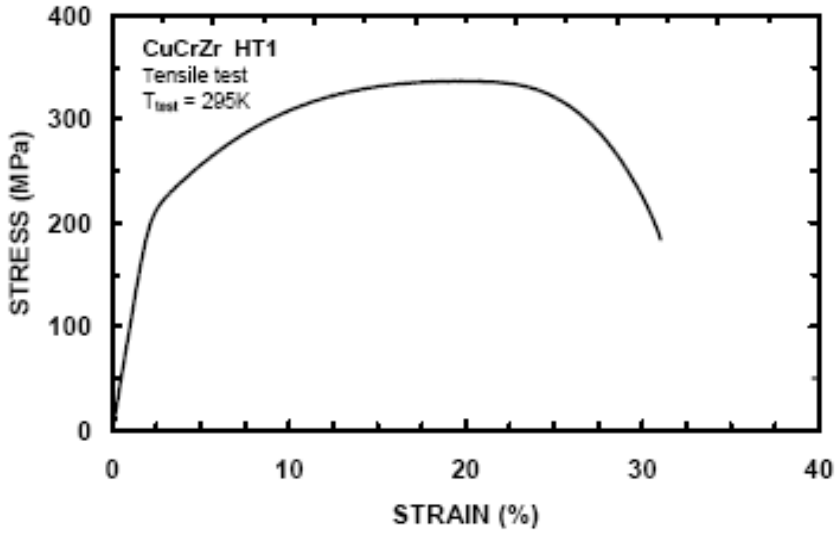

Figure 4. Stress-strain curve for the overaged CuCrZr (HT 1) alloy tested at 353K at a strain rate of $10^{-5}s^{-1}$ in the unirradiated condition. The test was performed on a specimen with the same size and geometry as used in the in-reactor tests and using a test module similar to that used in the in-reactor creep-fatigue tests.

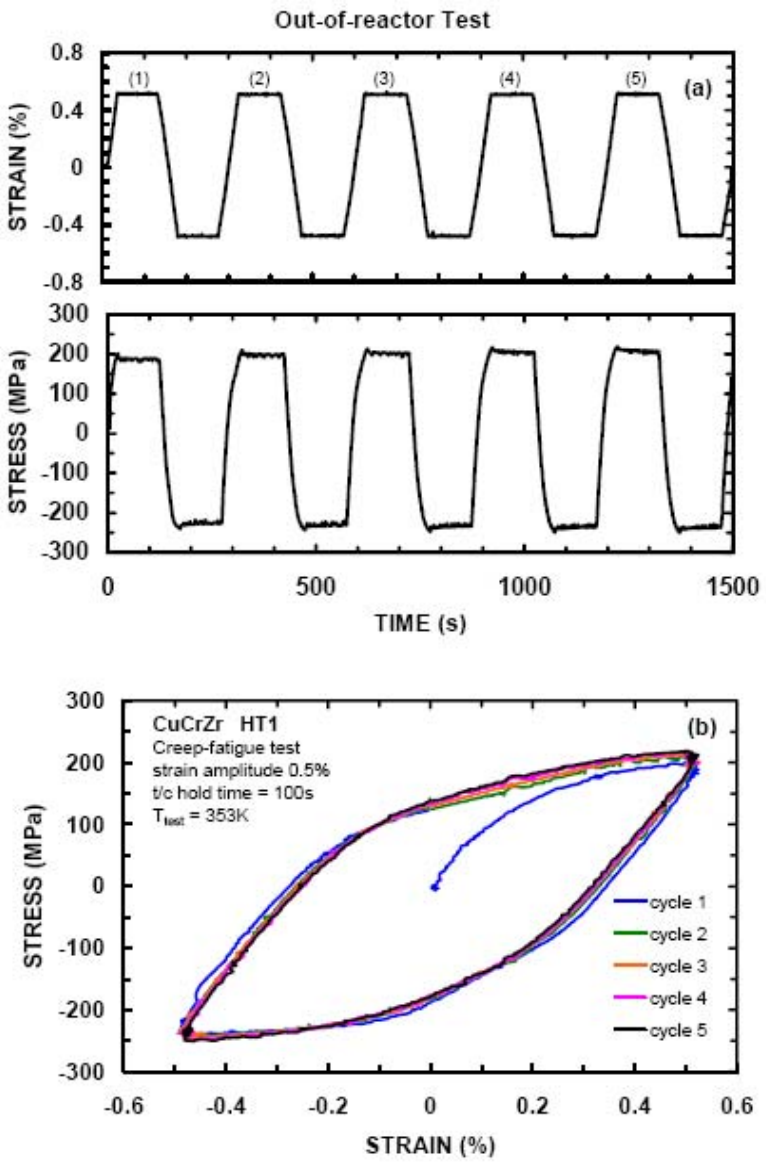

Figure 5. (a) Strain and stress response as a function of time and (b) cyclic deformation behaviour in the form of hysteresis loops obtained for different cycles during a creep-fatigue test performed at 353K on unirradiated overaged CuCrZr(HT 1) alloy with a strain amplitude of 0.5 % and a holdtime of 100s both in tension and compression sides of the loading cycles.

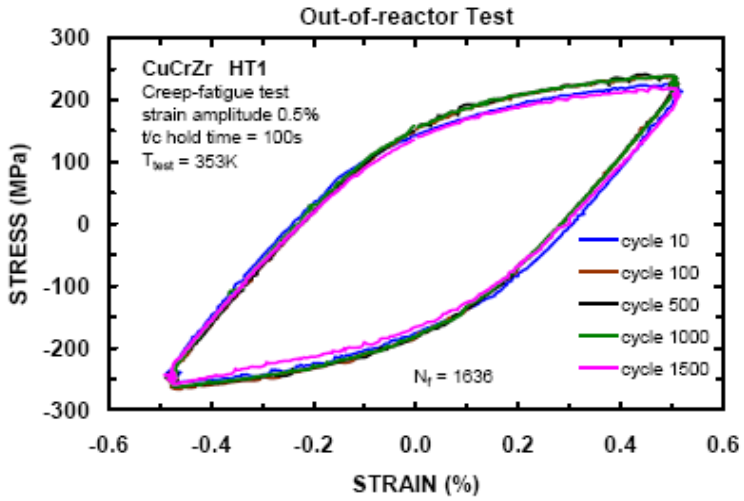

Figure 6. Same as in Figure 5(b) but for the higher number of creep-fatigue cycles representing increasingly higher level of deformation. The appropriate cycle numbers are indicated in the figure.

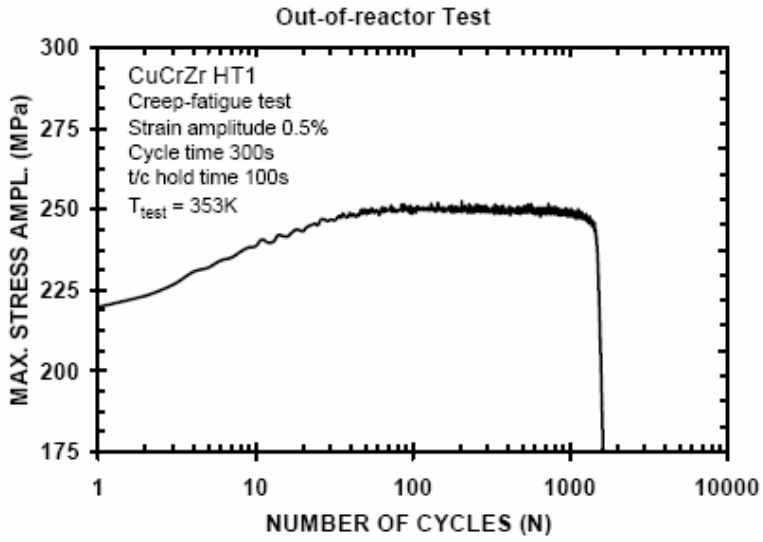

Figure 7. Variation of the maximum stress amplitude with the number of cycles during creep-fatigue test on the overaged CuCrZr(HT1) alloy at 353K with a strain amplitude of 0.5 %.The maximum stress amplitude is the average of the maximum tensile and compressive stresses recorded during each cycle.

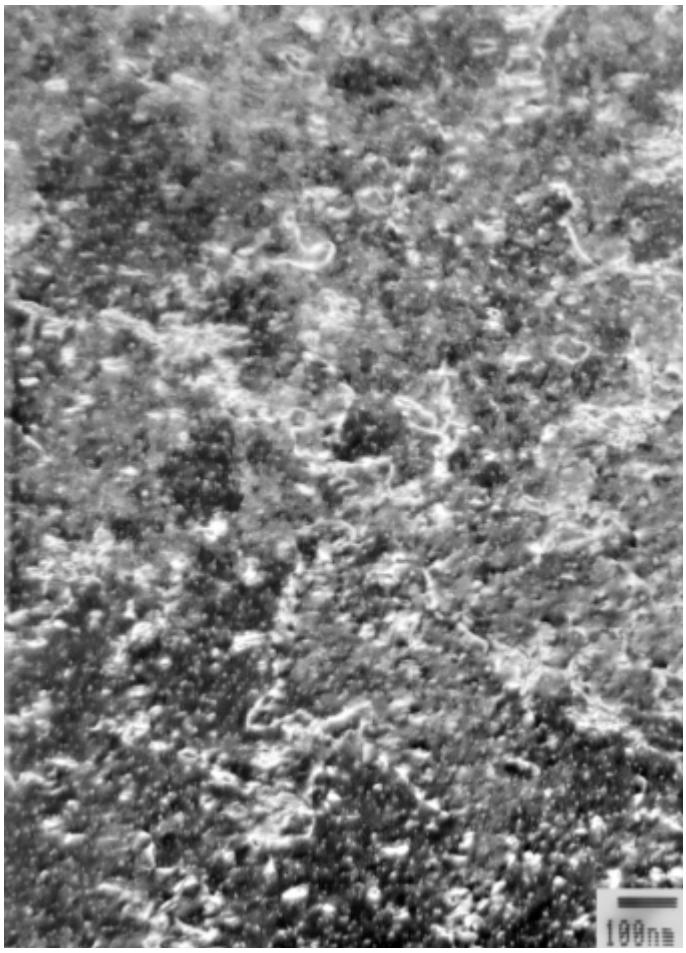

Figure 8. Post-deformation microstructure of CuCrZr (HT 1) alloy after out-of-reactor creep-fatigue testing (i.e. in the unirradiated condition) at 353K with a strain amplitude of 0.5 % and a holdtime of 100s.

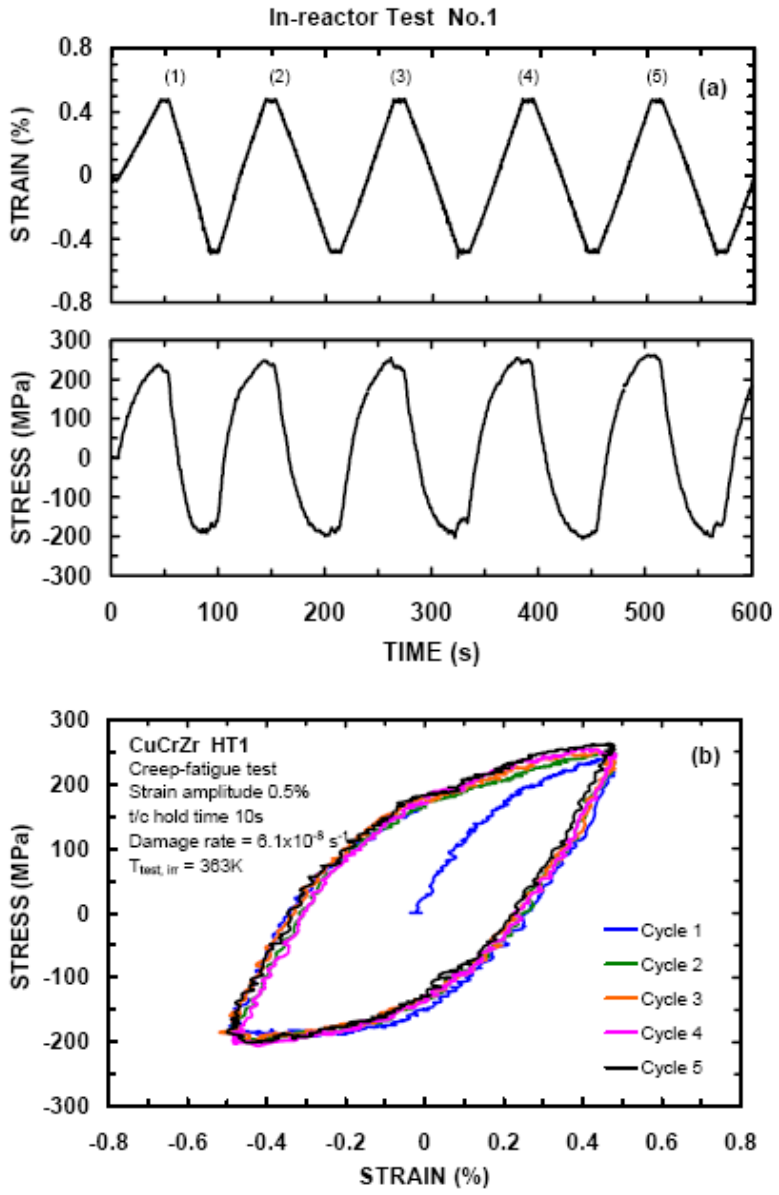

Figure 9. (a) Strain and stress response for the first five cycles as a function of test time and (b) cyclic deformation behavior in the form of hysteresis loops obtained for the same first five cycles shown in Figure 9 (a) during the in-reactor creep- fatigue test performed on CuCrZr (HT 1) specimen at 363K (Test No. 1, Module 2) with a strain amplitude of 0.5 % and a holdtime of 10 s both in tension and compression sides of the loading cycles.

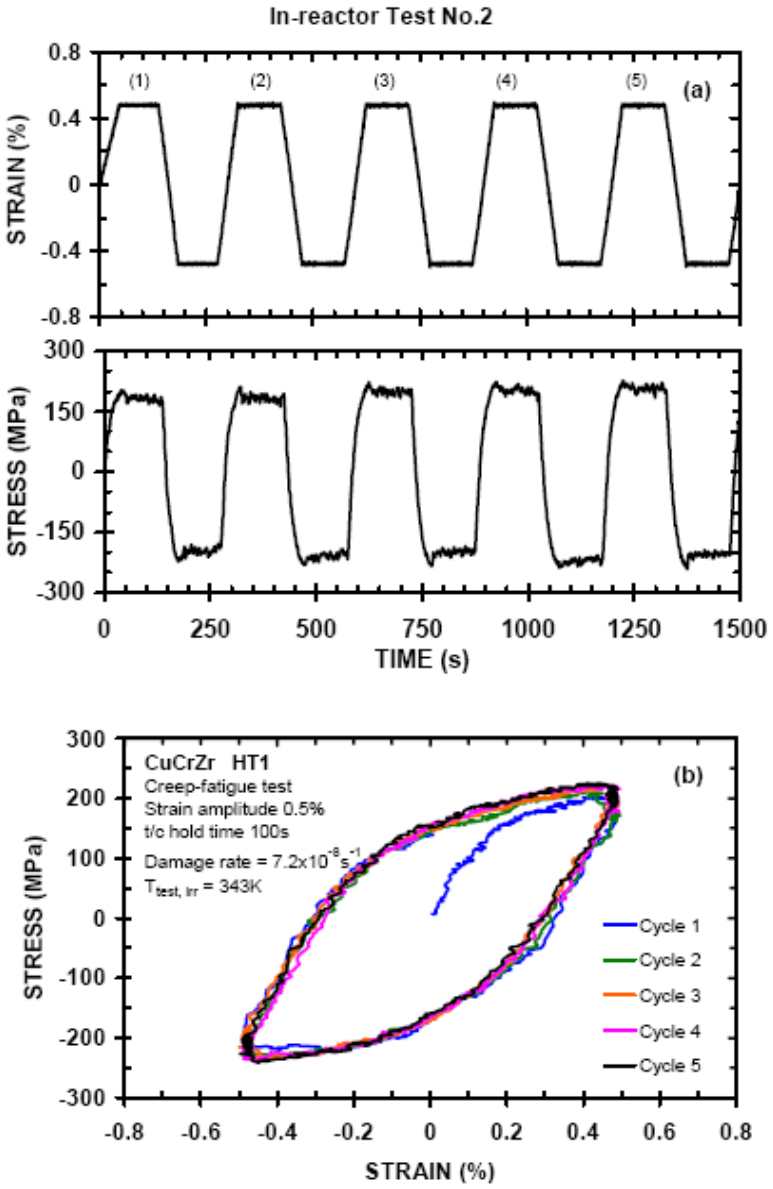

Figure 10. The same as in Figure 9 but for the test (Test No. 2, Module 1) carried out at 343K with a holdtime of 100s.

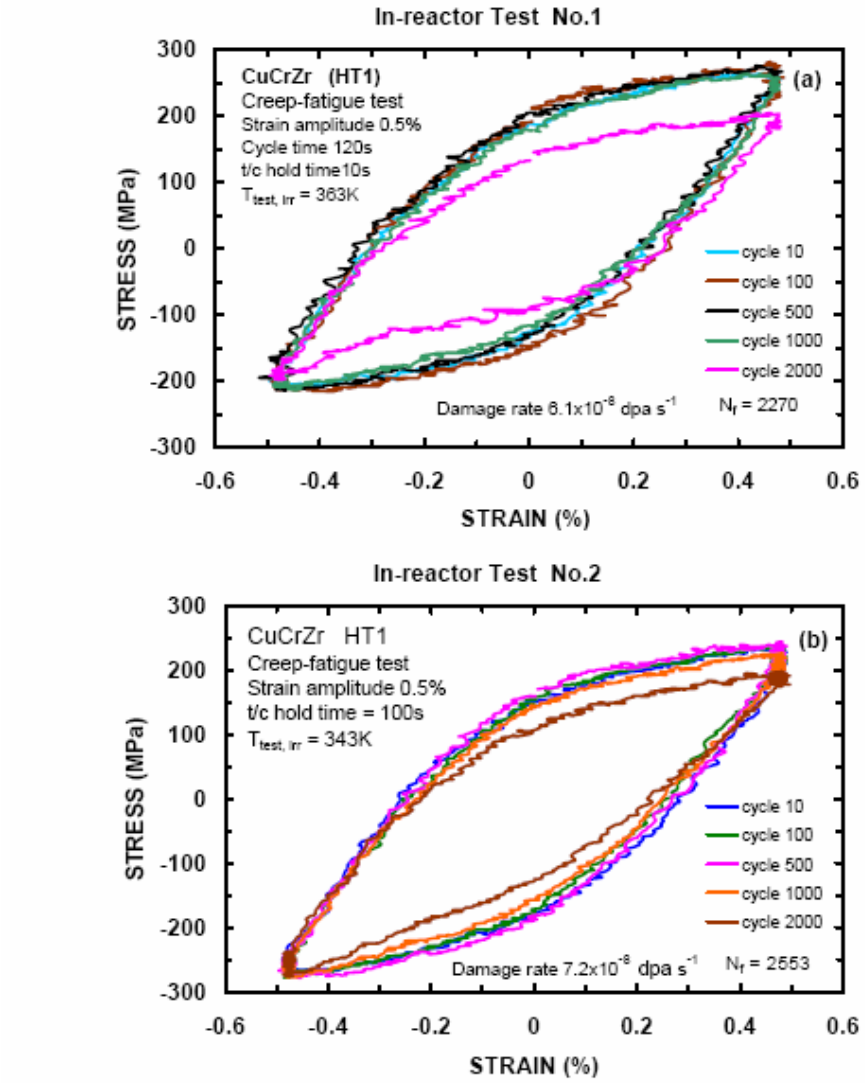

Figure 11.The cyclic deformation behavior in the form of hysteresis loops obtained for the higher number of creep-fatigue cycles representing higher level of deformation (and accumulated displacement dose) during the in-reactor creep -fatigue tests carried out at (a) 363K with a holdtime of 10s (Test No.1) and (b) at 343K with a holdtime of 100s (Test No.2). Both tests were carried out with a strain amplitude of 0.5 %.

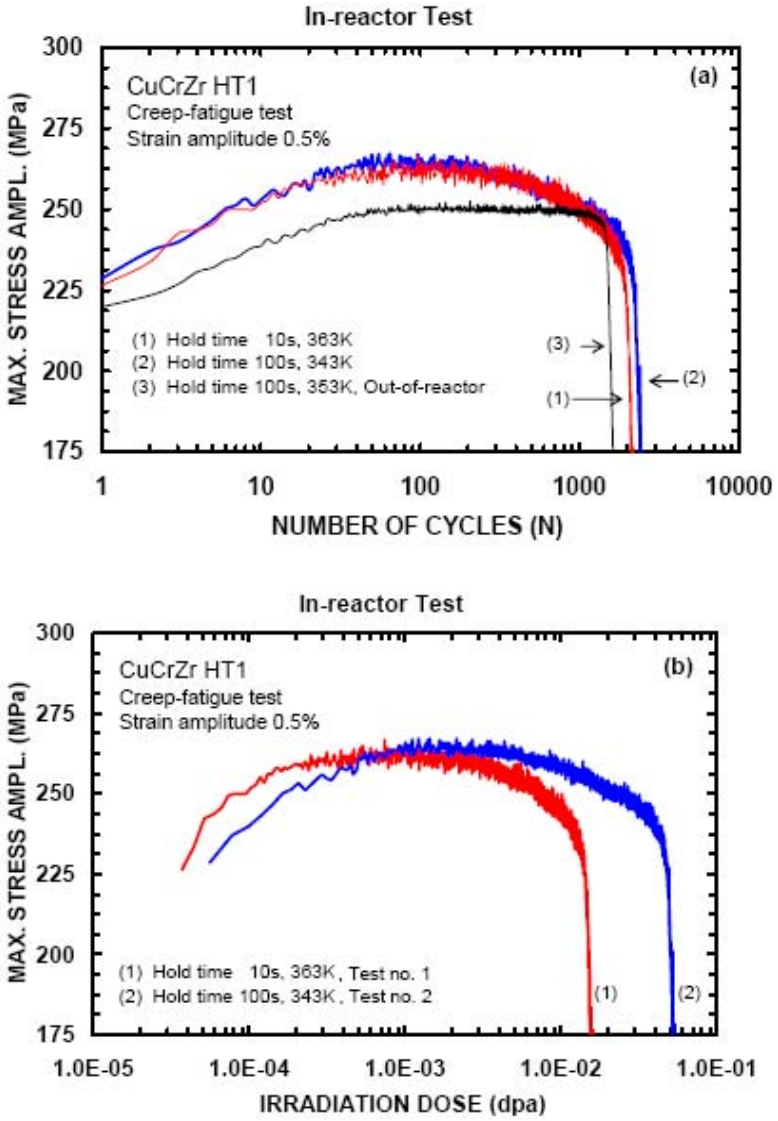

Figure 12.Variation of the maximum stress amplitude with (a) the number of cycles and (b) displacement dose during the in-reactor creep-fatigue tests carried out on CuCrZr (HT 1) specimens at 363 and 343K (Test No.1 and Test No.2, respectively)

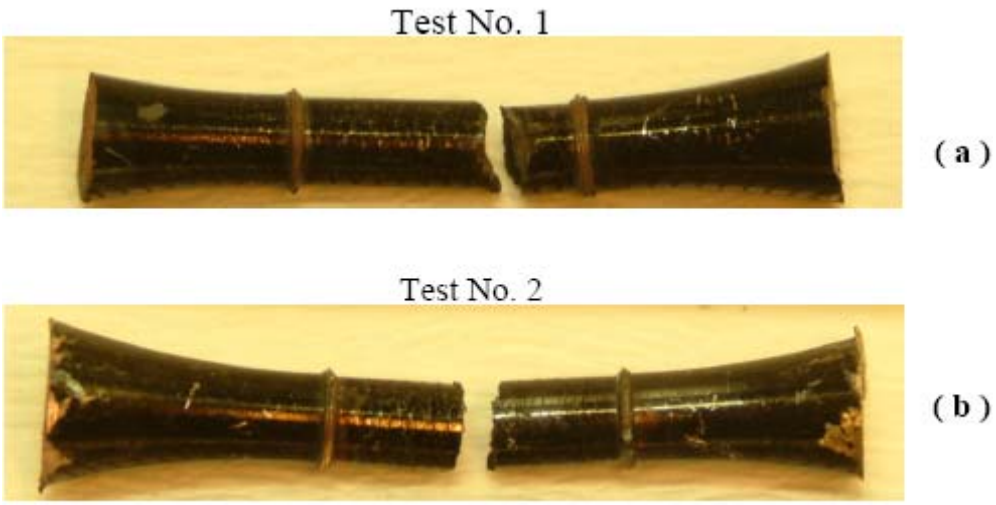

Figure 13. Photographs of the broken parts of the in-reactor creep-fatigue tested specimens used in (a) Test No. 1 and (b) Test No.2. None of the broken parts showed any evidence of necking of specimens prior to fracture

(a)

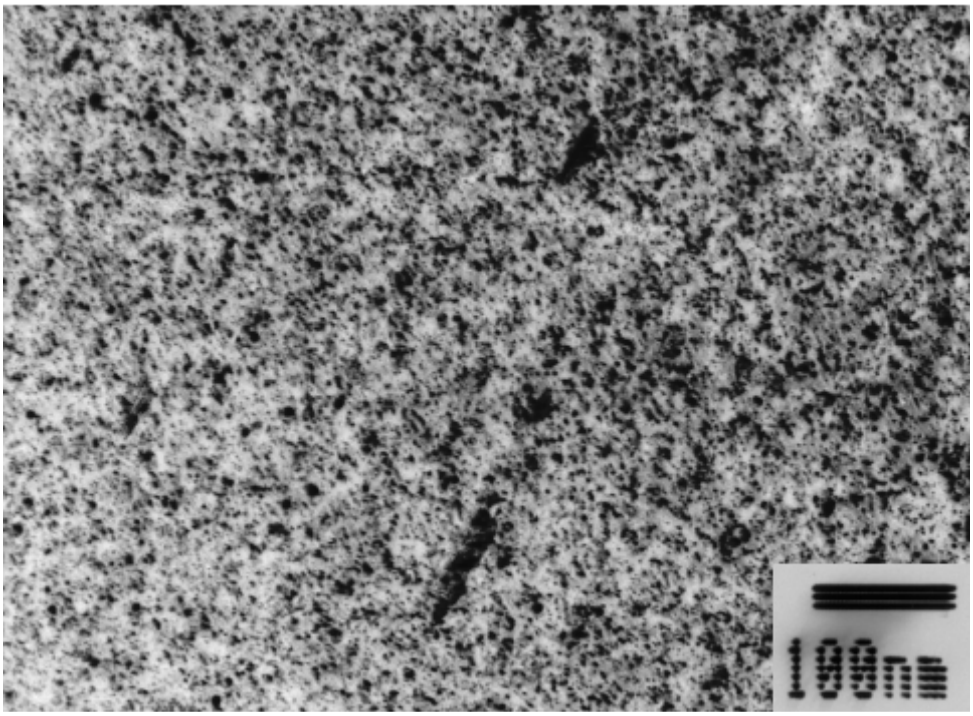

(b)

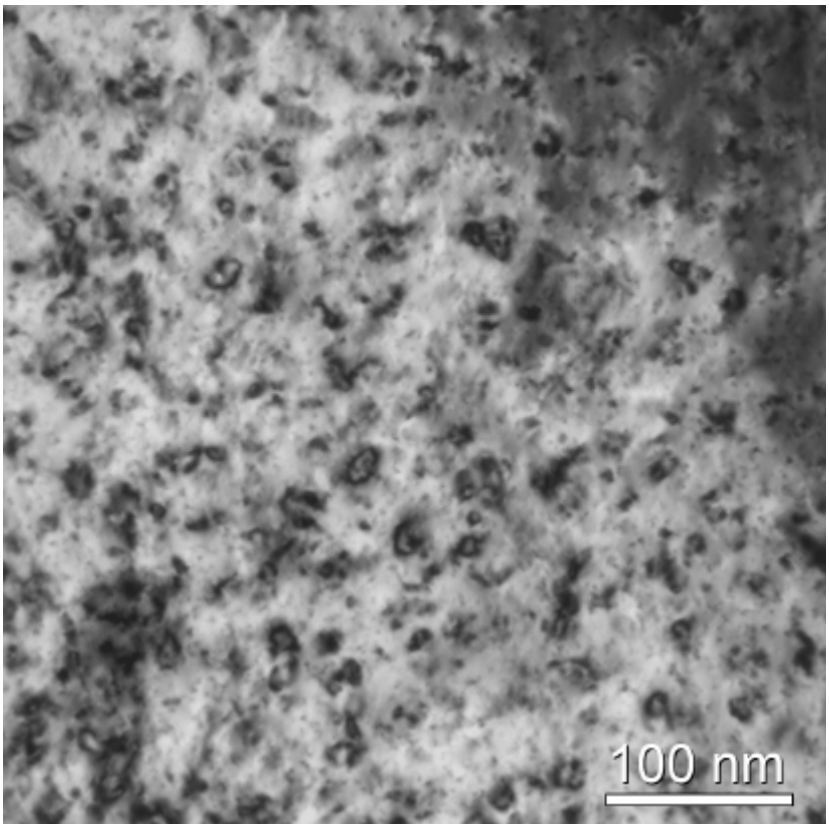

(c)

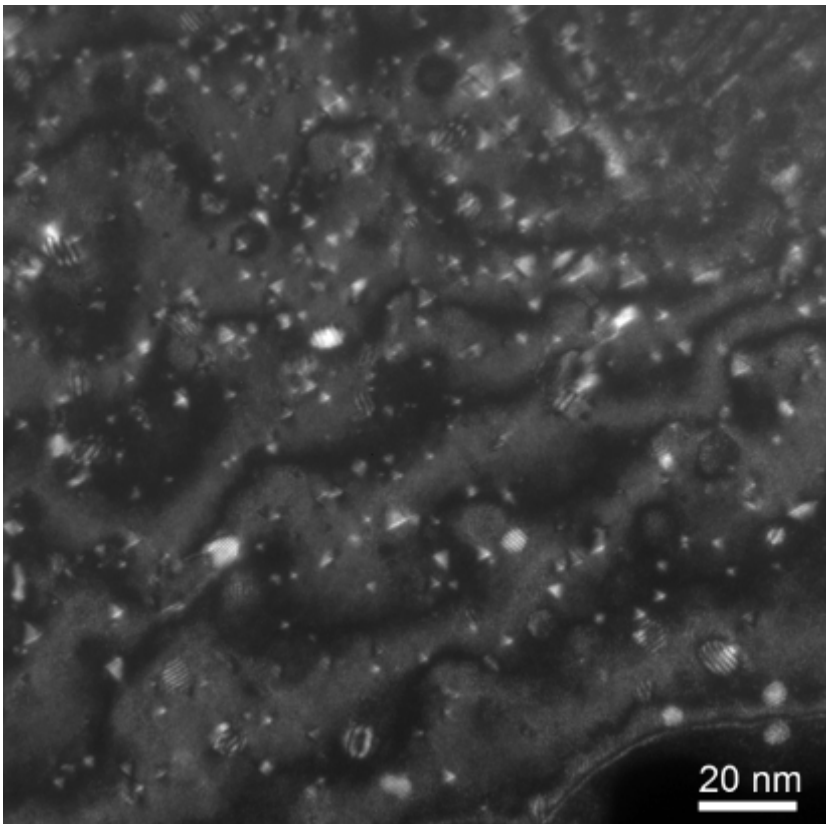

Figure 14. TEM micrographs showing precipitates and irradiation induced defect clusters in the overaged CuCrZr (HT 1) irradiated at 363K to a displacement dose level of 0.054 dpa in the absence of concurrent plastic deformation: (a) precipitates, SIA loops and SFTs at low magnification, (b) SIA loops and (c) precipitates and SFTs. The average densities and sizes of preciptates and SFTs are given in Table 2.

(a)

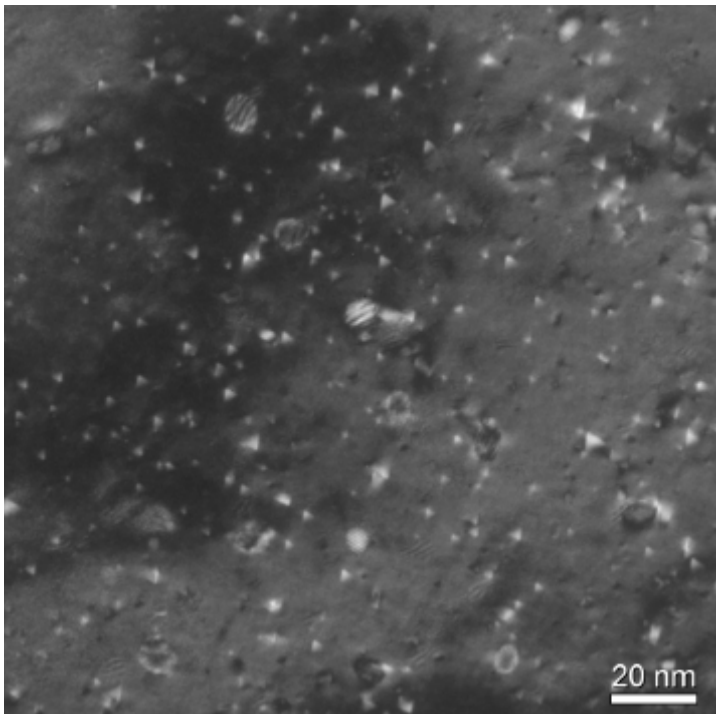

(b)

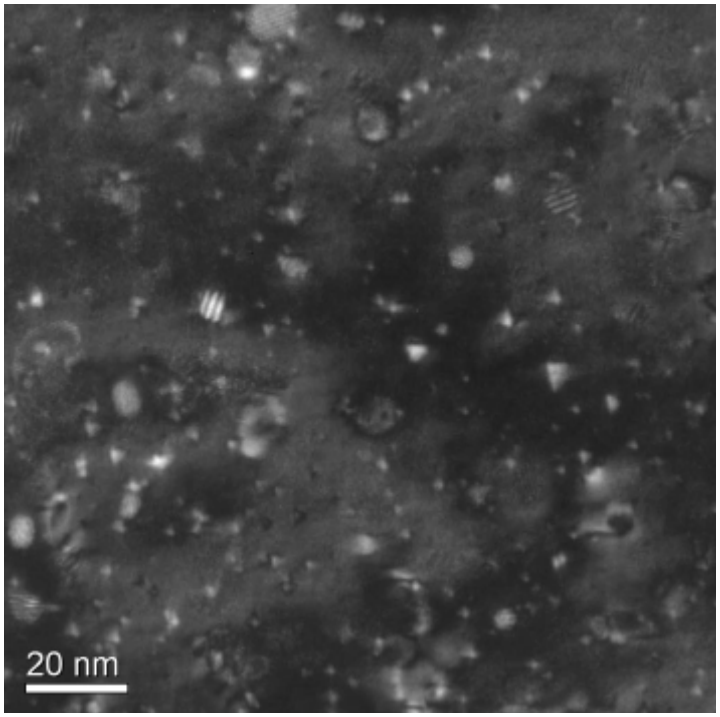

Figure 15 TEM micrographs showing the end of life microstructure of the in-reactor irradiated and simultaneously creep-fatigue tested specimens of CuCrZr(HT1) alloy with a strain amplitude of 0.5 % at (a) 363K(Test No.1) with a holdtime of 10s and (b) at 343K (Test No.2) with a holdtime of 100s. Note that the accumulated damage level during the actual creep-fatigue test period in the case of the Test No.1 was only 0.016 dpa. In the case of the Test No. 2, on the other hand, the damage accumulation was affected by the simultaneous creep-fatigue deformation during the whole irradiation period. The specimen in this test was exposed to neutrons producing a total displacement damage of 0.054 dpa (see Table 1).

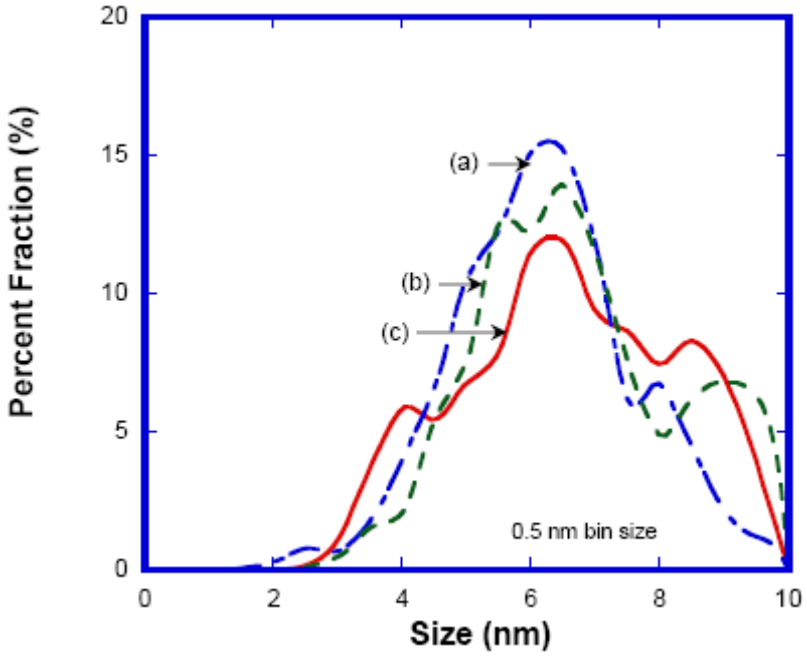

Figure 16. Precipitate size distributions in the overaged CuCrZr(HT1) alloy (a) in the irradiated and undeformed condition, (b) for the in-reactorTest No.1 and (c) for the in-reactor Test No. 2.

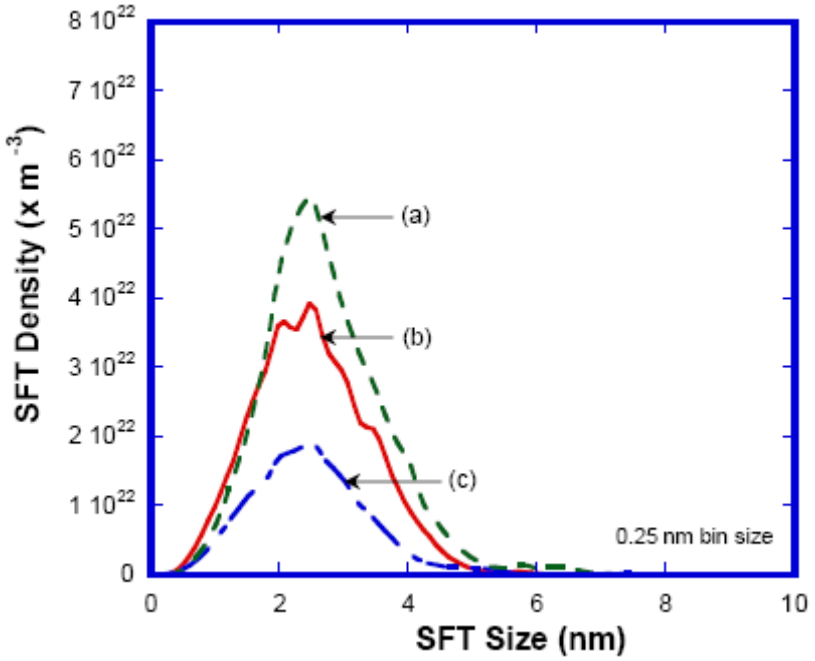

Figure 17. SFT size distributions determined for specimens in different conditions: (a) irradiated and undeformed, (b) irradiated and deformed in the in-reactor Test No.1 and (c) irradiated and deformed in the in-reactor Test No.2

(a)

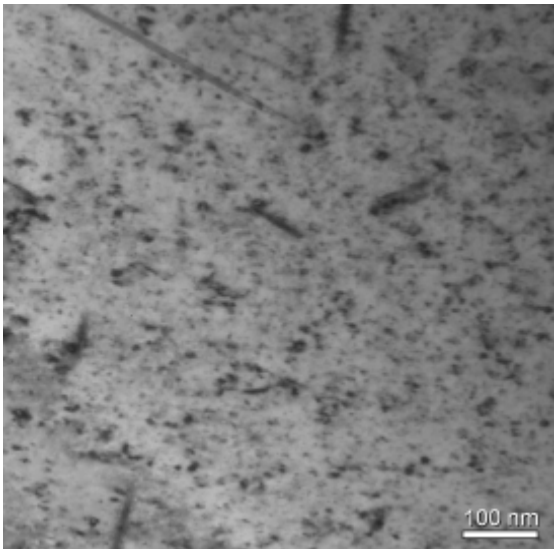

(b)

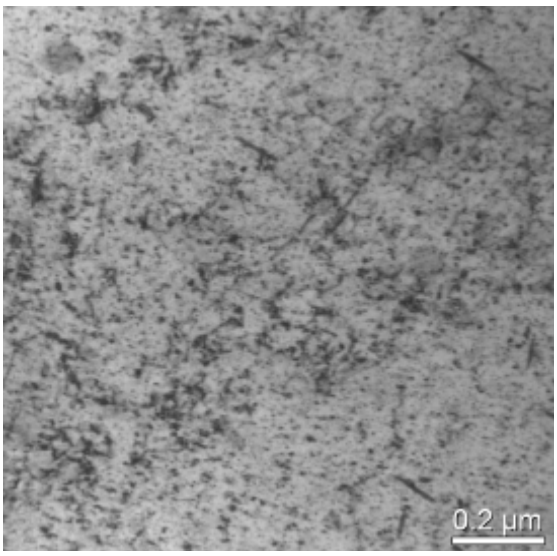

Figure 18. Dislocation microstructures of the in-reactor tested (Test No.1) specimen showing (a) homogeneous distribution of small loops and short dislocation segments and (b) dislocation segments and loops in group form.

(a)

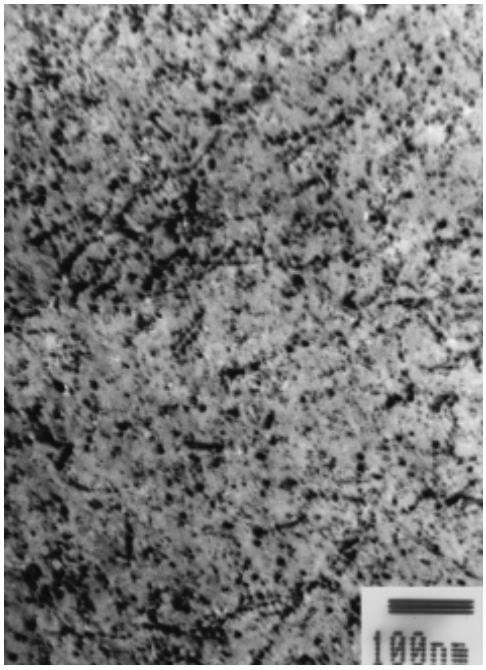

(b)

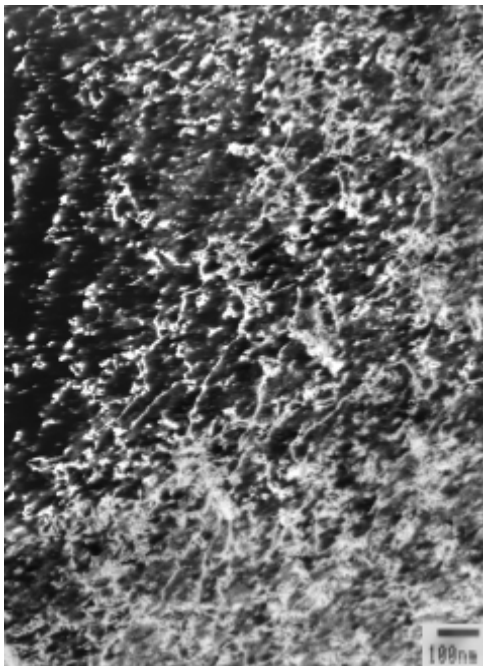

(c)

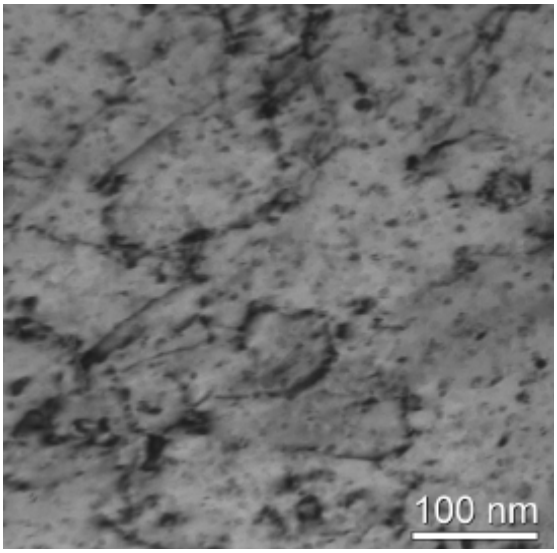

Figure 19. Dislocation microstructure in the in-reactor (Test No. 2) creep fatigue tested CuCrZr (HT1) specimen at 343k with a strain amplitude of 0.5%. The microstructure shows (a) loops and short dislocation segments often decorated with small loops, (b) longer dislocation lines and (c) loose groups of dislocations segments decorated by small loops.

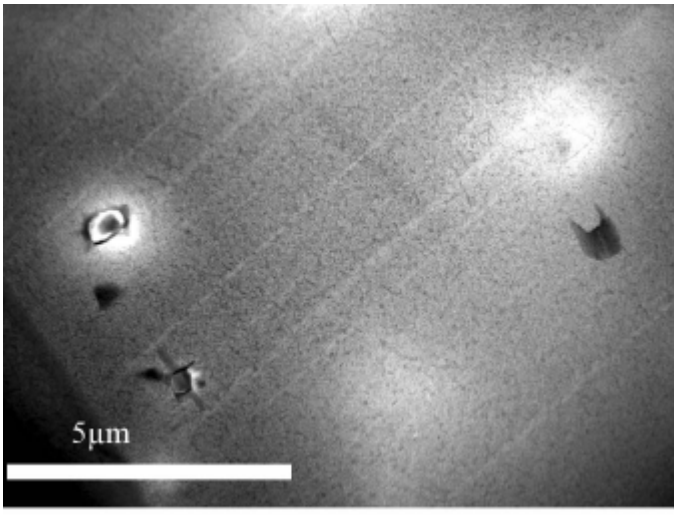

Figure 20. STEM micrograph taken from the specimen used in the in-reactor creep-fatigue test (Test No. 1) with a holdtime of 10s showing the formation of “diffuse” cleared channels (DCCs). Note that these channels appear to have eminated from a grain boundary.

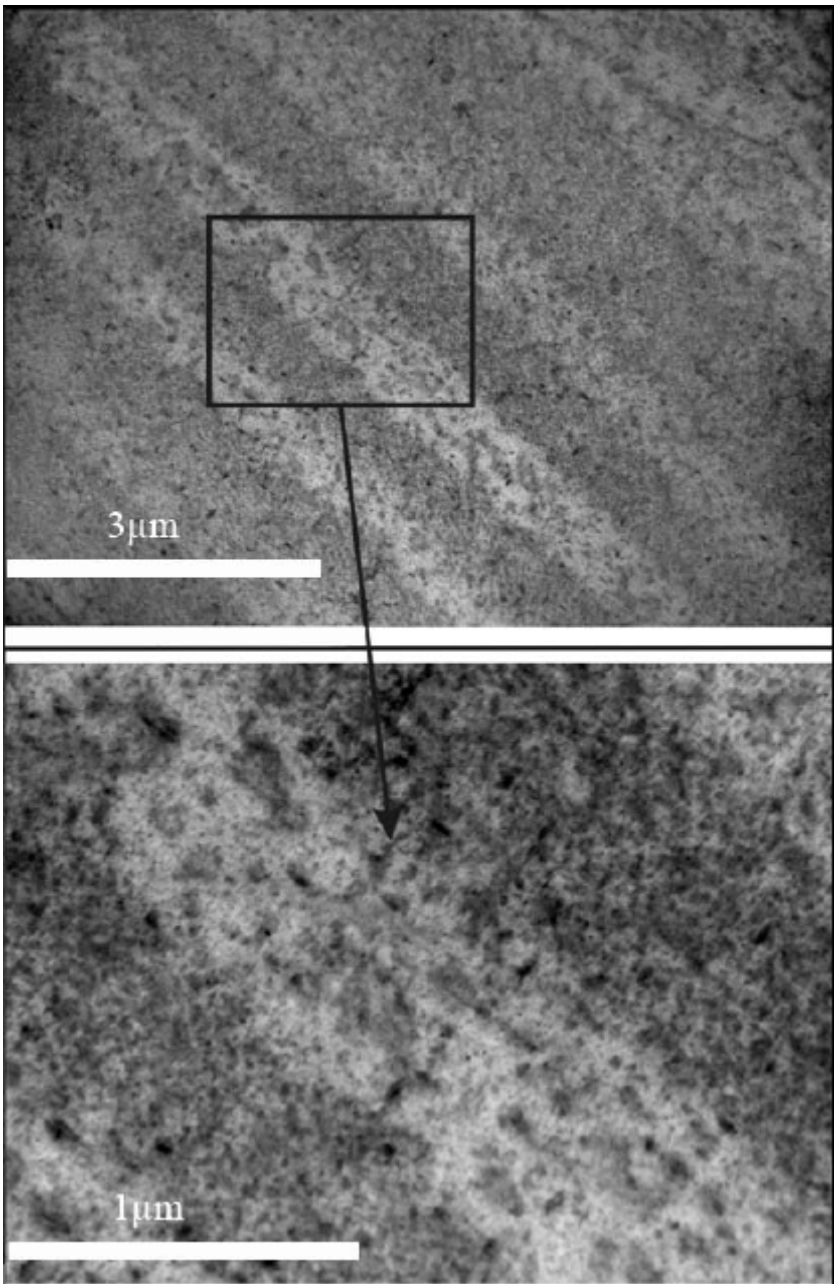

Figure 21. STEM micrographs taken from the specimen used in the in-reactor creep-fatigue test (Test No. 2) with a holdtime of 100s showing the formation of "diffuse" cleared channels (DCCs)

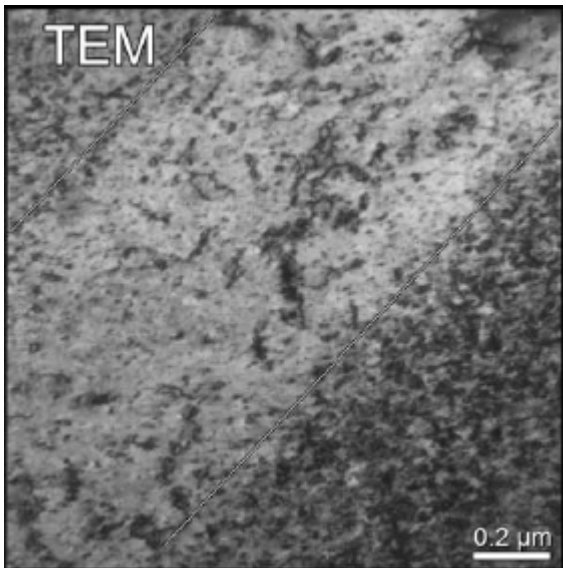

Figure 22 TEM micrograph taken from the specimen used in the in-reactor creep-fatigue test (Test No. 2) with a holdtime of 100s showing a “diffuse” cleared channel (DCC). Note that the channel contains some loops and small dislocation segments.

(a)

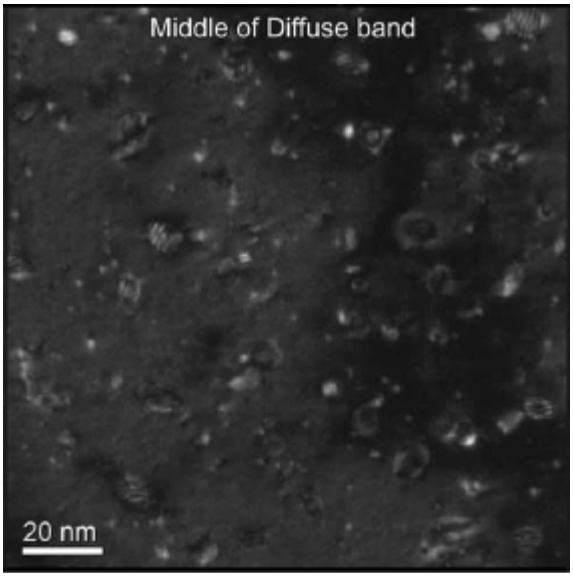

(b)

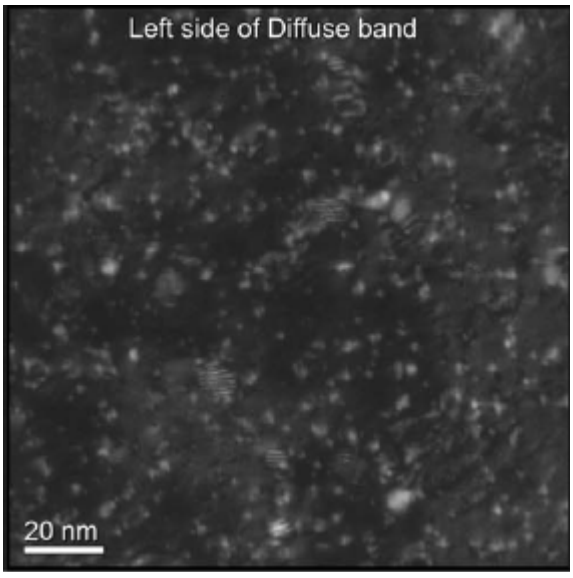

Figure 23 TEM micrographs illustrating the precipitate and SFT density (a) in the middle of a DCC and (b) in the neighbouring matrix in just out-side of the DCC in the specimen used in the in-reactor Test No. 2. Note that most of the SFTs in the middle of the DCC have been destroyed during the creep-fatigue deformation .

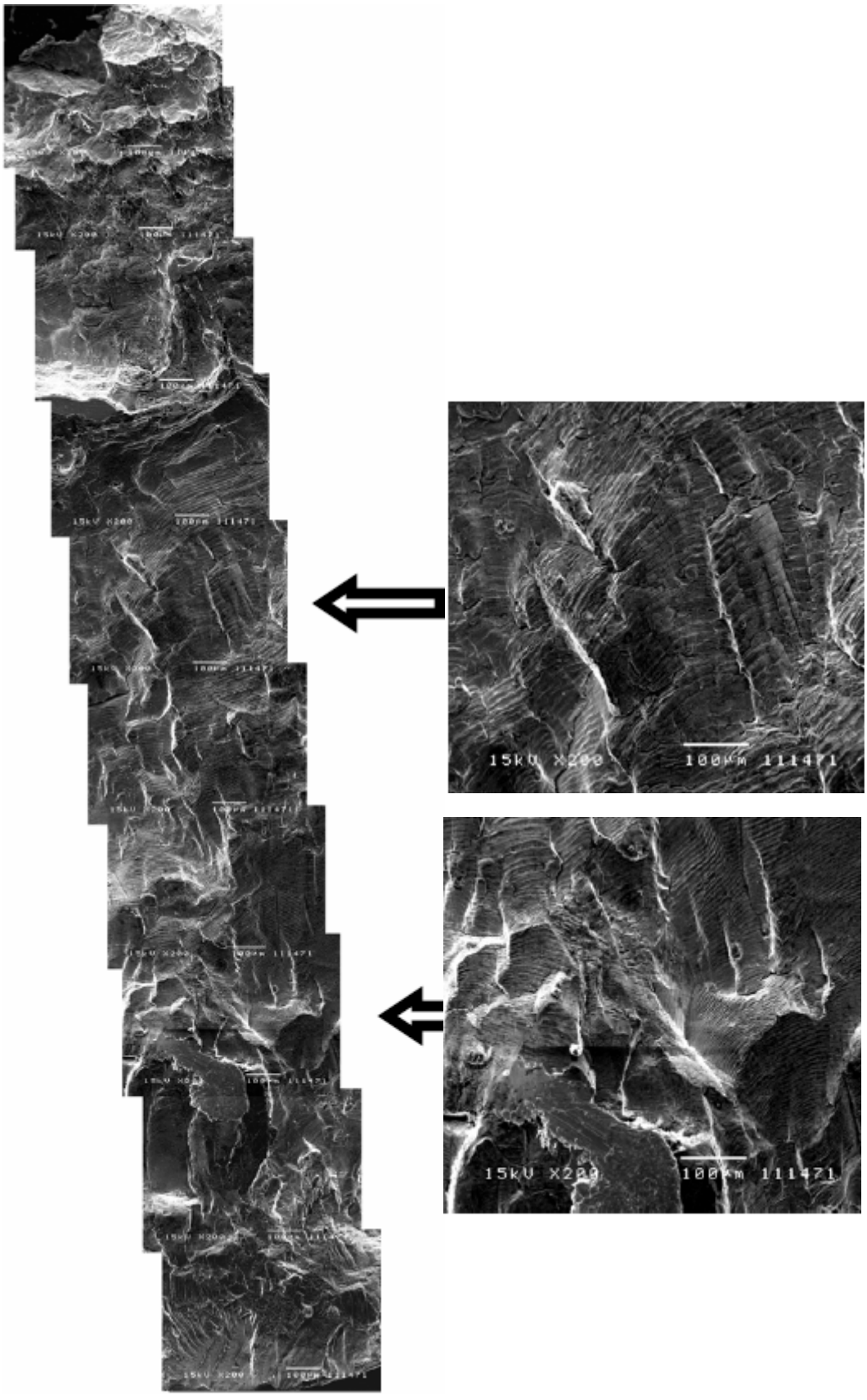

Figure 24 SEM fractograph illustrating fracture surface morphology for the unirradiated and out-of-reactor creep-fatigue tested at 353k with a strain amplitude of 0.5% and a holdtime of 100s.

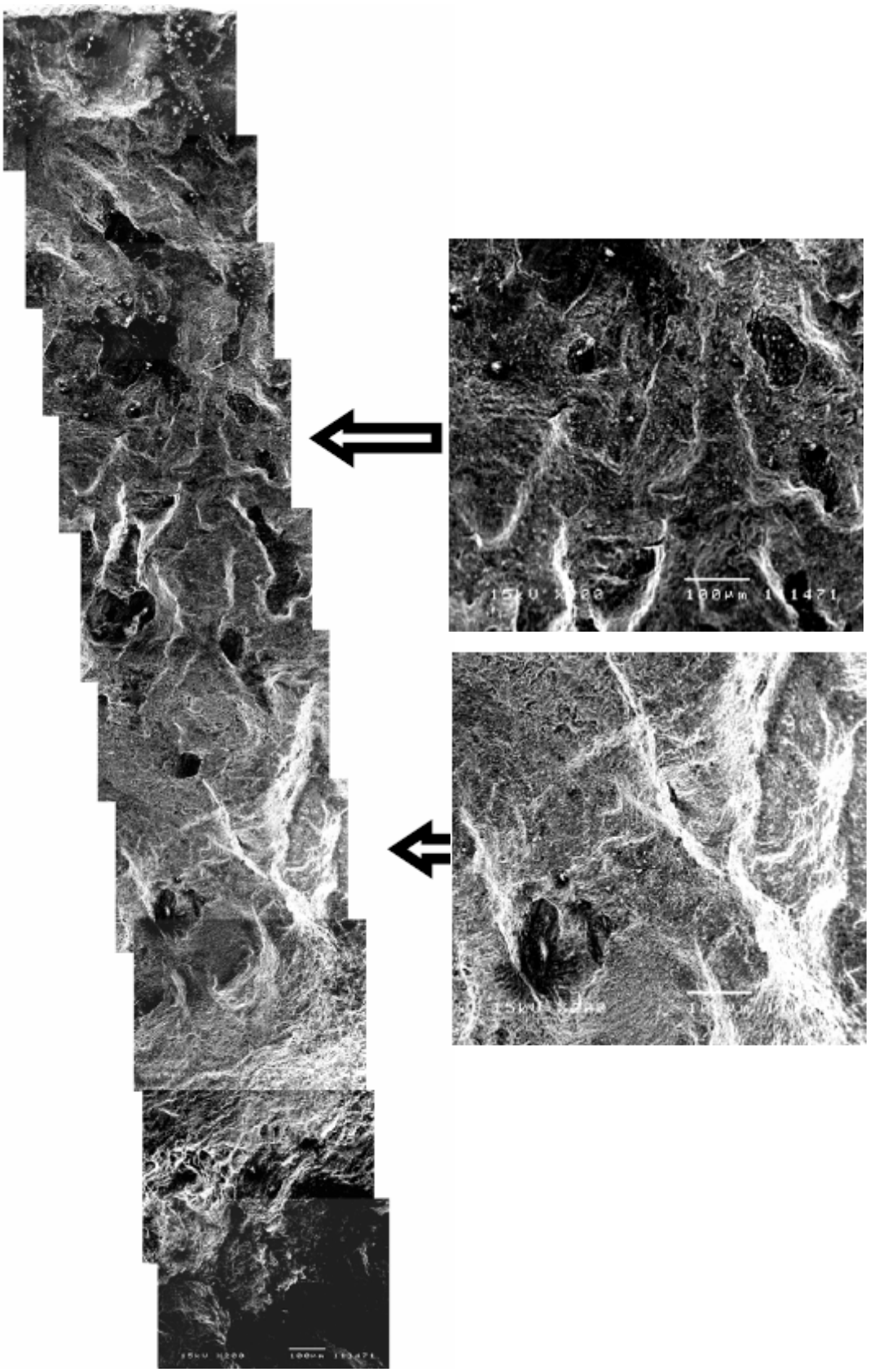

Figure 25 Same as in Figure 24 but for the specimen used in the in-reactor Test No. 1 carried out at 363k with a holdtime of 10s.

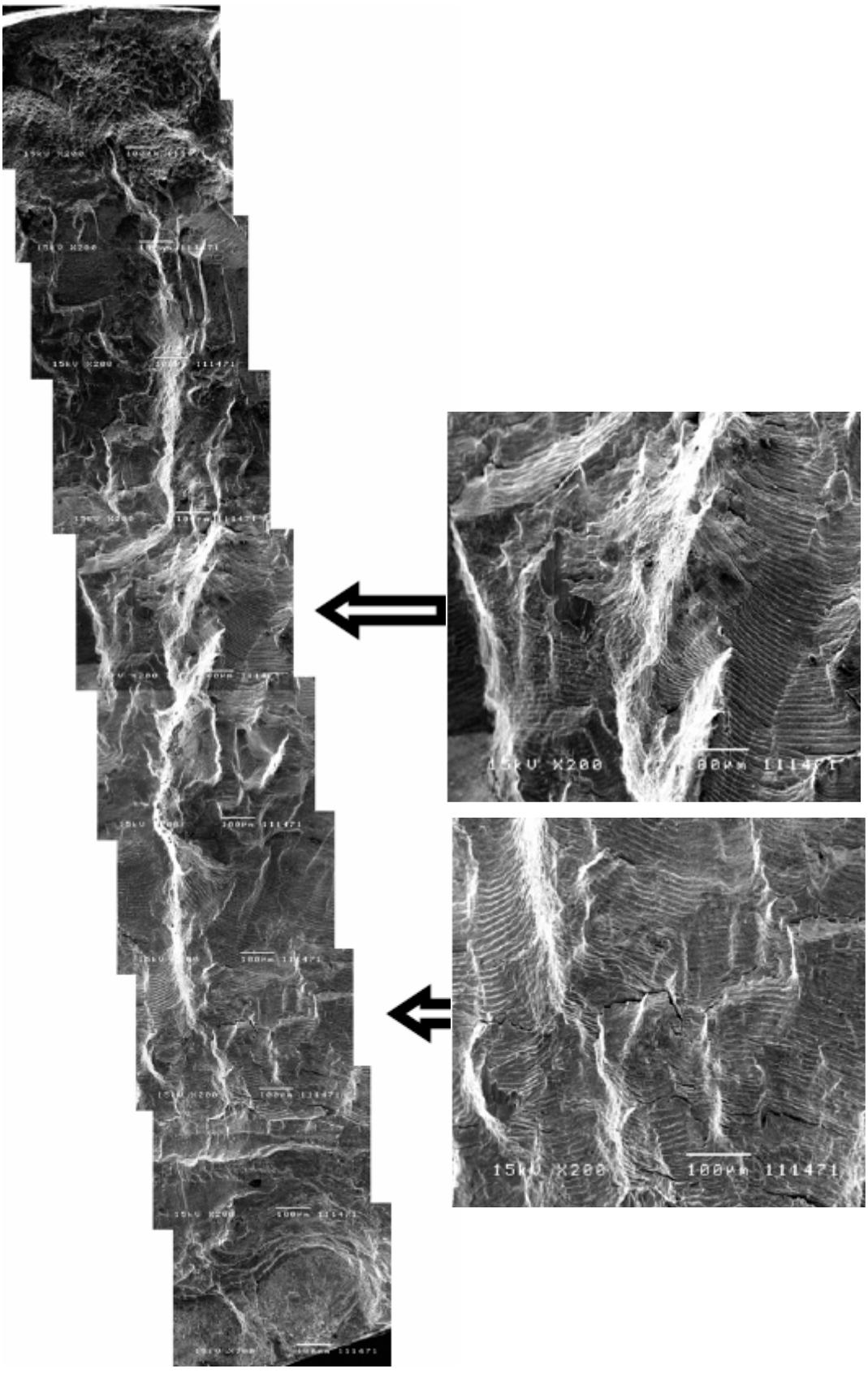

Figure 26 Same as Figure 25 but for the specimen used in the in-reactor Test No. 2 carried out at 343k with a holdtime of 100s.

Risø's research is aimed at solving concrete problems in the society.

Research targets are set through continuous dialogue with business, the political system and researchers.

The effects of our research are sustainable energy supply and new technology for the health sector.

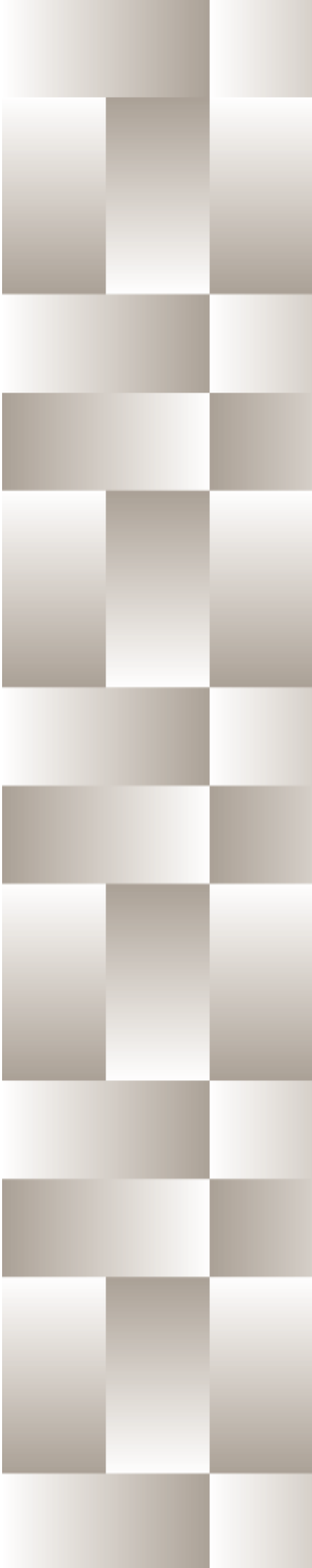

Risø-R-1571(EN)